# Activation of AMP-activated kinase at reperfusion protects the endothelial barrier against reperfusion-induced failure

**Inaugural Dissertation**

submitted to the

Faculty of Medicine

in partial fulfillment of the requirements

for the PhD-Degree

of the Faculties of Veterinary Medicine and Medicine

of the Justus Liebig University Giessen

By

**Muhammad Assad Riaz**

of

Mansehra, Pakistan

Giessen (2012)

From the Institute of Physiology

Director/Chairman: Prof. Dr. Rainer Schulz

of the Faculty of Medicine of the Justus Liebig University Giessen

First Supervisor and Committee Member: Prof. Dr. Thomas Noll
Second Supervisor and Committee Member: Prof. Dr. Andreas Dendorfer
Committee Members: Prof. Dr. Wolfgang Kummer and Prof. Dr. Stefen Arnhold

Date of Doctoral Defense: 03.12.2012

## Table of contents

**Abbreviations**

| | |
|---|---|
| AICAR | 5-aminoimidizole-4-carboxamide riboside |
| AJ | Adherens junctions |
| AMP | Adenosine monophosphate |
| AMPK | Adenosine monophosphate activated protein kinase |
| ANOVA | Analysis of variance |
| APS | Ammonium per sulfate |
| ASC | Association with Snf1 complex |
| ATP | Adenosine-5-triphosphate |
| Ara-A | Adenine 9-beta-d-arabinofuranoside |
| bFGF | Basic fibroblast growth factor |
| BSA | Bovine serum albumin |
| β-catenin | Beta catenin |
| °C | Degree celcius |
| $Ca^{2+}$ | Calcium |
| $CaCl_2$ | Calcium chloride |
| CaMKK | Calcium/CaM-dependent protein kinase kinase |
| cGMP | 3'-5'-cyclic guanosine monophosphate |
| cm/s | Centimeters per second |
| $CO_2$ | Carbon dioxide |
| CPI-17 | PKC-potentiated inhibitor 17-kDa protein |
| Ctr | Control |

| | |
|---|---|
| DMSO | Dimethyl sulfoxide |
| DTT | Dithiothreitol |
| ECL | Enhanced chemiluminescence |
| ECGS | Endothelial cell growth supplement |
| EC-MLCK | Endothelial cell myosin light chain kinase |
| EC | Endothelial cell |
| EDTA | Ethylene diamine tetraacetic acid |
| EGTA | Ethylene glycol-bis (2-aminoethylether)-N,N,N',N'-tetraacetic acid |
| EJ | Endothelial junctions |
| eNOS | Endothelial nitric oxide synthase |
| F-actin | Filamentous actin |
| FCS | Fetal calf serum |
| G-actin | Globular actin |
| GJ | Gap junctions |
| GLC | Germ line clones |
| GTP | Guanosine-5'-triphosphate |
| GTPases | Guanosine triphosphatase phosphohydrolase |
| H | Hypoxia |
| H11 K | protein H11 kinase |
| HBSS | Hanks' balanced salt solution |
| hEGF | Human epidermal growth factor |
| HEPES | 4-(2-hydroxyethyl)-1-piperazine ethane sulfonic Acid |

| | |
|---|---|
| HGF | hepatocyte growth factor |
| HR | Hypoxia-reperfusion |
| hrs | Hours |
| HUVEC | Human umbilical vein endothelial cells |
| IgG | Immunglobulin G |
| IgM | Immunglobulin M |
| IR | Ischemia-reperfusion |
| JAM | Junctional adhesion molecule |
| $K_{ATP}$ | Potassium ATP channel |
| KCl | Potassium chloride |
| kDa | Kilo dalton |
| $KH_2PO_4$ | Potassium dihydrogen phosphate |
| KIS | Kinase interacting sequence |
| LKB1 | Liver kinase B1 |
| MDCK | Madin-Darby Canine Kidney |
| $MgCl_2$ | Magnesium chloride |
| $MgSO_4$ | Magnesium sulphate |
| µM | Micromolar |
| MIF | Macrophage migration inhibition factor |
| min | Minutes |
| MLC | Myosin light chain |
| MLC~P | Phosphorylated myosin light chain |
| MLCK | Myosin light chain kinase |
| MLCP | Myosin light chain phosphatase |

| | |
|---|---|
| mM | Millimolar |
| mmHg | Millimeters of mercury |
| $MnCl_2$ | Manganese chloride |
| mPTP | Mitochondrial permeability transition pore |
| MYPT1 | Myosin phosphatase targeting subunit 1 |
| N | Normoxia |
| $N_2$ gas | Nitrogen gas |
| NaCl | Sodium chloride |
| $NaHCO_3$ | Sodium hydrogen carbonate |
| $Na_2HPO_4$ | Di-sodium hydrogen phosphate |
| $NaH_2PO_4$ | Sodium dihydrogen phosphate |
| Na-orthovanadate | Sodium orthovanadate |
| Neg siRNA | Negative small interfering ribonucleic acid |
| NF-κB | Nuclear factor κ-light chain enhancer of activated B-cells |
| NO | Nitric oxide |
| n.s. | not significantly different |
| p53 | Tumor suppressor protein 53 kDa |
| PBS | Phosphate-buffered saline |
| PFA | Paraformaldehyd |
| pH | Negative log of $H^+$ concentration |
| PI3K | Phosphoinositide 3-kinase |
| PKC | Protein kinase C |
| $Po_2$ | Partial pressure of oxygen |

| | |
|---|---|
| PP1 | Protein phosphatase 1 |
| RNA | Ribonucleic acid |
| ROS | Reactive oxygen species |
| S1P | Sphingosine 1-phosphate |
| Ser19 | Serine 19 |
| SD | Standard deviation |
| SDS | Sodium dodecyl sulfate |
| siRNA | Small interfering ribonucleic acid |
| SM-MLCK | Smooth muscle myosin light chain kinase |
| TAK1 | Transforming growth factor β-activated kinase1 |
| TBS | Tris-buffered saline |
| TEMED | N, N, N', N',-tetramethylethylenediamine |
| Thr172 | Threonine 850 |
| Thr18 | Threonine 18 |
| Thr38 | Threonine 38 |
| Thr850 | Threonine 850 |
| TJ | Tight junction |
| Tris | Tris (hydroxymethyl) aminomethane |
| TRITC | Tetramethyl Rhodamine Iso-Thiocyanate |
| VE-cadherin | Vascular endothelial cadherin |
| % vol/vol | Volume by volume percentage |
| % wt/vol | Weight by volume percentage |
| ZMP | 5-aminoimidazole-4-carboxamide-1-ribotide |
| ZO-1 | Zonula occluden 1 |

# Introduction

## 1.1 Endothelial cells and endothelium

Endothelium can be described as an organ system made up of a monolayer of endothelial cells (EC) that line the entire surface of the vascular system. In an average adult human body the cumulative weight of endothelium is several hundred grams, which serves as a selective barrier and, hence, controls the exchange of water, solutes, macromolecules and cells between the vessel lumen and interstitium (Michel and Curry, 1999). However, barrier function may fail under pathophysiological conditions such as hypoxia-reoxygenation (HR), which causes an extravasation of macromolecules and water finally leading to edema formation (Mehta and Malik, 2006).

It is well established that the equilibrium between cell-cell adhesive forces and actomyosin-mediated centripetal tension is essential for the regulation and stabilization of the vascular endothelial barrier integrity (Shen et al., 2009). Vascular endothelial (VE)-cadherin molecules are the major components of adherens junctions providing strong endothelial barrier properties and control the leakage of macromolecules through the paracellular pathway (Lampugnani et al. 1995). On the other side, contractile forces produced by the interactions of actomyosin pull adjacent EC apart (Goeckeler and Wysolmerski 1995), which facilitate the efflux of macromolecules across the endothelial barrier. Endothelial monolayers maintain a semipermeable barrier by controlling the equilibrium between adhesive and contractile forces. Dysfunction of endothelial barrier, vascular leakage and tissue edema occur if this equilibrium is disrupted (Garcia et al., 1995; Lum and Malik, 1996). Previous

studies have shown that EC injury in response to hypoxia or ischemia-reperfusion (IR) coinsides with contractile dysfunction in the myocardium, edema formation, vasoregulatory dysfunction, apoptosis and finally cell necrosis (Hansen, 1995; Scarabelli et al., 2001; Reffelmann et al., 2003). However, the processes that determine the protection against reperfusion injury are still not fully understood. AMP-activated protein kinase (AMPK) stimulation is known to protect the integrity of mitochondrial membrane potential and maintains the cellular energy levels, which makes this protein an extremely attractive pro-survival signaling mediator for protecting the cells and tissues against IR injury (Ido et al., 2002). Recently, several studies have documented that activation of AMPK can protect against IR injury both *in vitro* and *in vivo* (Gundewar et al., 2009, Shin et al., 2009, Paiva et al., 2009, 2010). Based on these studies it has been concluded that therapeutically targeting of this enzyme could be a promising novel strategy for treating diseases like angina, acute coronary syndrome or myocardial infarction.

In light of these observations the role of endothelial AMPK is analyzed in the present study. The central hypothesis is that AMPK is involved in the control of endothelial barrier function under physiological conditions and targeting AMPK activation can protect against an imminent barrier failure induced at the onset of reperfusion.

## 1.2 Endothelial barrier regulation

The key components that collectively regulate endothelial barrier function are endothelial cell-cell and cell-matrix adhesion proteins and the actiomyosin based contractile machinery. The adhesive strength is provided by a variety of junctional

proteins, which are associated with the actin cytoskeleton, and pevent the detachment of EC from the substratum or from its neighbor. This characteristic is the foundation that EC form a barrier that is able to controle the traffic of water, solutes, macromolecules and cells between the vascular lumen and the interstitial space. The role of different components in the regulation of endothelial barrier is discussed below.

### 1.2.1 Endothelial junctions

Endothelial junctional complexes comprise adherens junctions (AJ), tight junctions (TJ) and gap junctions (GJ). AJ and TJ are responsible for the physical attachment between the EC and thus maintain the restrictiveness of endothelial barrier (Dejana et al. 2008). GJ are intercellular channels and required for the communication between neighboring EC. They allow the passage of water, ions and other small molecules between coupled cells. AJ are formed through homophilic interaction of transmembrane VE-cadherins, which are anchored intracellularly to the actin cytoskeleton via α, β, and γ-catenins. Additionally, p120 protein is another important regulatory component of cadherin adhesive complex that plays an important role in stabilization of cadherins at the cell membrane by modulating its membrane trafficking and degradation. TJ are composed of transmembrane proteins such as occludin, claudins, and junctional adhesion molecules (JAM), linked intracellularly to actin cytoskeleton through zonula occluden 1 (ZO-1) (Komarova et al., 2007).

### 1.2.2 Endothelial actomyosin cytoskeleton

Microfilaments are one of the major structural components that make up the endothelial cytoskeleton. Actin is the main building block of microfilaments and,

therefore, plays a very important role in the regulation of endothelial permeability (Shasby et al., 1982; Phillips et al., 1989; Schnittler et al., 1990). Actin exists in a monomeric form, known as G-actin, as well as in a filamentous form, called F-actin (Tobacman and Korn, 1983). It has been reported that actin together with the motor protein myosin comprise approximately 16% of total EC protein (Schnittler et al., 1990).

Actin fibers may be localized in bundles adjacent to the cell membrane. This cortical actin assembly is linked to specific cell-cell adhesion protein complexes and is of particular importance for maintenance of the integrity of endothelial barrier by tightning cell contacts between adjecant endothelial cells. There is accumulating evidence that the effect of drugs like sphingosine 1-phosphate (S1P), hepatocyte growth factor (HGF), and high molecular weight hyaluronate on cortical actin ring formation is causally linked with stabilization of endothelial barrier and protection (Garcia et al., 2001; Singleton et al., 2006, 2010). As described by Bogatcheva and Verin (2008), such process seems to be regulated by the contribution of a number of proteins that are involved in nucleation, bundling, branching and capping of actin.

In contrast to a cortical assembly, actin and myosin may form filament bundles, called stress fibers, which are major elements of contractile cytoskeletal structures (Dudek and Garcia, 2001; Vouret-Craviari et al., 1998). Previous studies indicate the critical role of actin polymerization in endothelial contraction and increased permeability response (Alexander et al., 1988; Fasano et al., 1995; Phillips et al., 1989; Schaphorst et al., 1997; Vouret-Craviari et al., 2002). Ermert et al. (1995, 1997) have reported the disruption of actin cytoskeleton in response to C2 toxin that induced changes in cell shape, permeability and edema formation in lung. Inflammatory mediators like thrombin promotes robust actin stress fiber formation that led to the contraction and development

of isometric force in different cell types (Kolodney and Wysolmerski, 1992). Likewise, HR-induced endothelial permeability changes have been shown to be accompanied by increased actin polymerization and formation of stress fibers (Lum et al., 1992; Torii et al., 2007) suggesting a key role of actin in the regulation of endothelial barrier permeability.

## 1.3 Endothelial contractile machinery

It is well documented that contractile machinery of EC is driven primarily by the interaction between actin and myosin, which is mainly controlled through myosin light chain (MLC) phosphorylation. MLC, myosin light chain kinase (MLCK) and myosin light chain phosphatase (MLCP) are the major regulators of the contractile machinery that are briefly discussed below.

### 1.3.1 Myosin light chain

It is well established that the increase in macromolecular permeability of endothelial monolayers by various mediators is due to an intercellular gap formation, a process which is partly controlled through phosphorylation of the regulatory light chain of myosin (Schnittler et al., 1990; Wysolmerski and Lagunoff, 1991; Sheldon et al., 1993; Lum and Malik, 1994; Garcia et al., 1995). MLC is a 20 kDa protein which after its phosphorylation controls the actin-myosin interaction causing force generation and cell retraction (Wysolmerski and Lagunoff, 1991; Kamisoyama et al., 1994). MLC phosphorylation and contractile activation is shown also to be involved in the induction of hyperpermeability in response to IR. Previous studies have demonstrated in cultured endothelial monolayers that IR elicits the activation of the contractile

machinery, which, in conjunction with disruption of cell–cell junctions, leads to intercellular gap formation, loss of endothelial barrier function and myocardial edema formation (Gündüz et al., 2006; Kasseckert et al., 2009).

### 1.3.2 Myosin light chain kinase

Endothelial cell MLCK (EC-MLCK) is a $Ca^{2+}$/calmodulin (CaM)-dependent enzyme that phosphorylates MLC at Ser19 and/or Ser19/Thr18 (Garcia et al., 1995; Hixenbaugh, 1997; Moy et al., 1993; Verin et al., 1998). It is generally acknowledged that MLCK gets activated via $Ca^{2+}$-dependent mechanisms in response to inflammatory mediators, resulting in an increase in MLC phosphorylation followed by endothelial cell retraction and endothelial permeability (Sheldon et al., 1993). Both, the 214 kDa EC-MLCK and the smaller 130 – 150 kDa smooth muscle MLCK (SM-MLCK) isoforms are encoded by a gene located on chromosome 3 (Dudek and Garcia, 2001). The EC-MLCK is structurally similar to SM-MLCK with an additional unique 922 amino acid N-terminal domain containing consensus sites phosphorylated by several protein kinases (Garcia et al., 1997; Verin et al., 1998). Wysolmerski and Lagunoff (1991) have initially discussed the role of MLCK in the regulation of barrier permeability via phosphorylating MLC in permeabilized bovine pulmonary artery endothelial monolayers. Subsequent studies have further elaborated the essential role of MLCK in the regulation of permeability using both *in vitro* and *in vivo* approaches (Sheldon et al., 1993; Garcia et al., 1995; Khimenko et al., 1996; Yuan et al., 1997; Parker, 2000; Wainwright et al., 2003).

### 1.3.3 Myosin light chain phosphatase

Along with MLCK, MLCP is involved in the regulation of the phosphorylation state of MLC in EC. Verin et al. (1995) have demonstrated that inhibition of the protein phosphatase 1 (PP1), the catalytical subunit of MLCP, increased MLC phosphorylation and cell contraction. Whereas, MLC phosphorylation was markedly reduced and actin-myosin interaction was clearly disturbed when PP1 was microinjected in cytoplasm of mammalian fibroblasts (Fernandez et al., 1990). MLCP is a holoenzyme that consists of three subunits, a 37 kDa catalytic subunit PP1, a 110-130 kDa myosin phosphatase targeting subunit 1 (MYPT1) and a small 20 kDa subunit with yet unknown function (Hartshorne et al., 1998). In EC the δ isoform of PP1 is predominantly found to be associated with MYPT1 in the MLCP holoenzyme (Verin et al., 2000; Härtel et al., 2007), which is an essential catalytic phosphatase in smooth muscle MLCP, too. In smooth muscle cells PP1 binding to the N-terminus of MYPT1 promotes its activity, resulting in the dephosphorylation of MLC, which critically determines the physical and functional integrity of MLCP (Hubbard and Cohen, 1993; Johnson et al., 1997). In addition, various studies have demonstrated several other distinct mechanisms that are involved in the regulation of MLC phosphatase activity (Kimura et al., 1996; reviewed by Hartshorne, 1998). MYPT1 was shown to be involved in the formation of an active MLCP complex by targeting PP1 to its substrate myosin. Formation and activity of MLCP is regulated by phosphorylation of MYPT1 at Thr696 and Thr850. There is considerable evidence that phosphorylation at these sites of MYPT1 causes MLCP inhibition (Feng et al., 1999; Velasco et al., 2002; Kimura et al., 1996), which can subsequently result in increased MLC phosphorylation.

The exact mechanism of MLCP inhibition following phosphorylation of MYPT1 is not yet clear. To our current understanding, phosphorylation of MYPT1 occurs in the C-terminal half and PP1 binds to the N-terminal of the molecule, suggesting that the folding of MYPT1 protein takes place in such a way that the phosphorylation site comes closer to or interacts with PP1. Another study suggests that conformational changes in quaternary structure might be involved in both processes, i.e activation and inhibition of phosphatase (Ito et al., 2004). In fact, nearly all reported models in previous studies seam speculative and further data is needed to clarify the exact mechanism involved in the inhibition of MLCP through MYPT1 phosphorylation. Another mechanism involved in the regulation of MLCP is through protein kinase C-potentiated inhibitory protein for PP1 of 17 kDa (CPI-17) (Eto et al., 1995). In addition to known PKC-dependent phosphorylation, CPI-17 is also phosphorylated by Rho kinase at Thr38 that directly binds to PP1Cδ and inhibits the MLCP holoenzyme activity (MacDonald et al., 2001; Kitazawa et al., 1999).

## 1.4 AMP-activated protein kinase

### 1.4.1 AMPK structure

AMP-activated protein kinase (AMPK) is a heterotrimeric enzyme consisting of a catalytic α subunit, regulatory β and γ subunits that are expressed in many mammalian tissues (Towler and Hardie, 2007). A serine/threonine protein kinase catalytic domain resides in the N-terminal half of the α subunit, whereas the C-terminal half is involved in binding the β and γ subunits, which is a prerequisite for AMPKαβγ complex formation. Truncation and site-directed mutagenesis in different functional domains of the AMPKα1 subunit is known to abolish the formation of this αβγ

complex, which leads to the inactivity and instability of AMPK (Crute et al., 1998). In addition to a poorly conserved N-terminal domain, the AMPK β subunit has a kinase interacting sequence (KIS) and association with Snf1 complex (ASC) regions that are highly conserved in all eukaryotes. Recent studies have revealed that only the ASC domain of β subunit is specifically required for the assembly of AMPKαβγ complex whereas KIS domain is involved in the glycogen binding. The γ subunit of AMPK contains a N-terminal region and four cystathionine beta synthase (CBS) domains commonly referred to as *"Bateman domains"* that are conserved between γ subunits, which represent the binding sites for AMP and ATP (Hardie et al., 2003). Studies have shown that multiple genes like α1, α2, β1, β2, γ1, γ2, γ3 encode different isoforms of each AMPK subunit that can produce 12 heterotrimeric complexes of the enzyme (Hardie, 2004). The expression of all these isoforms in mammals emphasizes the existence of a large family of AMPK complexes *in vivo* (Towler and Hardie, 2007). However, the effects of alterations in specific AMPK isoforms on the enzyme activity have not yet been thoroughly investigated in relation to their particular localization and specific downstream targets.

### 1.4.2 AMPK function in energy metabolism

It is generally believed that the major source of energy to carry out basic cellular functions is ATP, whose concentration is typically 1–10 mM in the cell (Beis and Newsholme, 1975). For the normal metabolic processes, concentration of the cellular ATP must be maintained within a very narrow range that is achieved through a proper regulation of anabolic and catabolic pathways, cellularly as well as systemically. Previous studies have revealed that this co-ordination can be accomplished by AMPK

signaling that is known as cellular energy sensor acting as a metabolic master switch (Winder and Hardie, 1999; Hardie et al., 2003). Accumulating evidence indicates that elevation of AMP triggers a conformational change in the γ subunit of AMPK leading to a strong activation of this kinase. Two molecules of AMP bind to two *Bateman domains* located on the γ subunit with positive cooperativity, thereby exposing the active site on the α subunit to upstream kinases (Hardie, 2004; Scott et al., 2004). Further validation of this mechanism is done by using 5-aminoimidazole-4-carboxamide-1ß-riboside (AICAR), an AMPK agonist that is widely used to activate AMPK in several experimental settings. AICAR is taken up by cells through adenosine transporters and phosphorylated by adenylate kinase to produce an AMP mimetic 5-aminoimidazole-4-carboxamide-1-ribotide (ZMP) inside the cell (Merrill et al., 1997). Binding of AMP to the γ subunits increases the activity of AMPK and promotes the phosphorylation of Thr172 that is located in its activation loop, a region where many kinases need phosphorylation for their activation (Johnson et al., 1996). Several groups have demonstrated that AMPK phosphorylation at Thr172 is essential for its activity (Crute et al., 1998; Stein et al., 2000; Hawley et al., 1996) and this activity mirrors phosphorylation status of the AMPK at Thr172 (Carling, 2004).

Numerous studies have suggested that metabolic or environmental stress factors like hypoxia, ischemia, glucose deprivation, prolonged exercise and heat shock lead to activation of AMPK (Marsin et al., 2000; Kudo et al., 1995; Musi et al., 2001; Winder and Hardie, 1996; Corton et al., 1994). Such conditions ultimately decrease the intracellular ATP levels and increase those of AMP, which lead to the activation, and phosphorylation of AMPK. Additionally, the AMPK is further phosphorylated and activated by upstream kinases mainly by liver kinase B1 (LKB1) (Hawley et al., 1996)

and calcium/CaM-dependent protein kinase kinase (CaMKK) (Woods et al., 2005; Hurley, 2005) (Fig 1.1). Other studies indicate that AMPK can also be phosphorylated by transforming growth factor β-activated kinase 1 (TAK1) in certain cells (Momcilovic et al., 2006). Additionally, AMP binding to the γ-subunit of AMPK also prevents its dephosphorylation by protein phosphatases, while increasing concentrations of ATP blocks the AMPK activity by preventing the AMP binding to the kinase (Sanders et al., 2007).

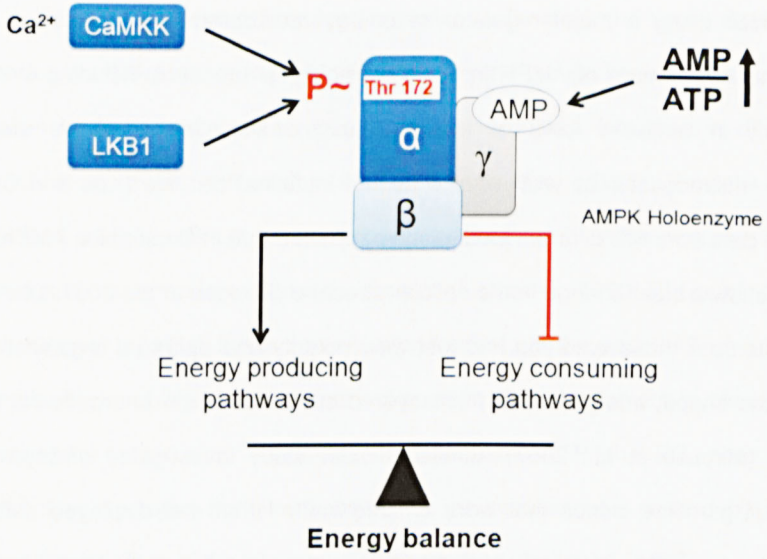


**Fig. 1.1** The structure and regulation of AMPK: AMPK is heterotrimeric complex, composed of three subunits (α, β, γ) that is activated by upstream kinases i.e. CaMKK and LKB1 through phosphorylation of Thr172 in its α subunit. Binding of AMP to the γ subunit allosterically activates the AMPK, which consequently leads to its increased phosphorylation. LKB1 is an upstream kinase which, in opposite to CaMKK, is activated independently of intracellular calcium concentration. AMPK restores the energy balance by switching on energy producing pathways (catabolic processes) while switching off energy consuming pathways (anabolic processes) upon its activation.

### 1.4.3 AMPK function in cell structure

Besides being a major regulator of energy metabolism, recent studies have revealed the involvement of AMPK in other physiological functions including structure and polarity in epithelial cells of lower organisms like *Caenorhabditis elegans*, Drosophila melanogaster as well as in a human intestinal cell line (Koh and Chung, 2007). The data from two different studies have reported that in Drosophila, AMPKα null mutations show a clear change in the cellular structure (Mirouse et al., 2007; Lee et al., 2007). Cells from these embryos had lost their polarity and epithelial organization by changing the shape, and produced multi-layered structures under energetic starvation conditions (Mirouse et al., 2007). Similarly, other study investigated embryos from AMPKα null germline clones that were embryonically lethal and displayed deformed cuticular structures devoid of ventral denticle belts and defective epithelium. Moreover, they also indicated irregular distribution of multiple polarity markers such as Bazooka (an apical complex marker), β-catenin (an adherens junction marker) and Discs-large (a basolateral marker) throughout the epithelia (Lee et al., 2007).

Beneficial effects of targeted AMPK activation in the regulation of epithelial tight junction assembly have also been discussed in Madin-Darby canine kidney (MDCK) cells (Zheng and Cantley, 2007; Zhang et al., 2006). Expressing a dominant–negative mutant of AMPKα led to tight junction disassembly, delayed relocation of ZO-1 to cell junctions, diminished transepithelial electric resistance and increased paracellular permeability in response to a temporal calcium withdrawal followed by readdition of calcium to the culture medium ("calcium switch"; Zhang et al., 2006). Hence, besides coordinating the energy status, AMPK also seems to be involved in other fundamental cellular processes including cell architecture.

## 1.5 Hypoxia-reperfusion

Many studies have examined vascular dysfunction and tissue damage following reperfusion of hypoxic or ischemic tissues. Several groups have shown that reperfusion causes an increased vascular permeability and edema formation in different organs (Lynch et al., 1988; Patt et al., 1988; Khimenko et al., 1996). Previous reports have indicated a rapid edematous swelling of myocardium in saline-perfused hearts during reperfusion, independent of blood elements (Noll et al., 1999; Di Napoli, 2001). These data suggest a partial, but extremely important role of the endothelium in the control of vascular permeability of the coronary circulation. Possible factors involved in increased permeability under such conditions may be extrinsic to the EC, such as ischemic metabolites secreted from cardiomyocytes or intrinsic, i.e., caused by the impaired energy metabolism of the coronary EC themselves (Noll et al., 1995).

There is general agreement that endothelial barrier function becomes progressively impaired during pathalogical conditions like HR (Inauen et al., 1990; Witt et al., 2003; Lum et al., 1992). This impairment of endothelial barrier function may occur due to activation of the contractile machinery, derangement of the actomyosin cytoskeleton and opening of intercellular gaps (Gündüz et al., 2006; Schäfer et al., 2003) (Fig 1.2), the processes clearly associated with increased endothelial permeability and edema formation (Lum and Malik, 1996; McDonald et al., 1999). Therefore, the integrity of the endothelium is an absolute necessity for the proper functioning of the vascular system especially under the pathological conditions including ischemia, hypoxia, stroke, diabetes and inflammatory diseases.

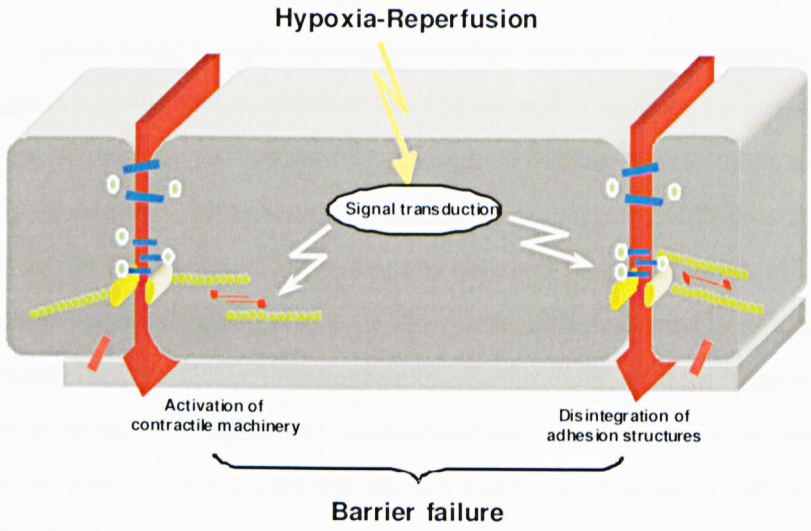


**Fig.1.2** Schematic diagram showing the mechanism of endothelial barrier failure during hypoxia-reperfusion. Pathophysiological conditions like ischemia/hypoxia and reperfusion cause impairment of endothelial barrier function by provoking a cascade of intracellular signals that effect on the contractile machinery, actin cytoskeleton and the cell-cell adhesion structures.

## 1.6 Hypoxia-reperfusion and AMPK pathway

As mentioned before, AMPK performs appropriate functions to maintain cellular energy homeostasis under various stress conditions. Once activated, AMPK inhibits energy-consuming anabolic pathways and stimulates catabolic pathways that increase energy supply by generating ATP. Thus, manoeuvres activating AMPK might have the potential to prevent myocardial injury under conditions of metabolic stress, by

maintaining the cellular energy homeostasis. In line with that, several studies have shown that activation of AMPK reduces IR-associated apoptosis, necrosis and infarct size in the myocardium as well as in other organs, whereas inhibition of AMPK activity enhanced tissue injury (Russell et al., 2004; Wang et al., 2009). Activation of AMPK by short term caloric restriction improved left ventricular recovery after IR (Shinmura et al., 2005). Likewise, AMPK activation in course of a cardioprotective intervention called ischemic preconditioning provides cardioprotection against reperfusion-induced injury (Sukhodub et al., 2007).

Pharmacological activation of AMPK by the anti-diabetic drug metformin has also been reported to protect against reperfusion-induced myocardial injury (Calvert et al., 2008; Gundewar et al., 2009). These studies showed that chronic activation of AMPK, beginning at the onset of reperfusion, significantly improved left ventricular function and survival in a murine model of heart failure. Recent progress shed light on various AMPK activators and their cardioprotective capability including AICAR, adiponectin, macrophage migration inhibition factor (MIF), and protein H11 kinase (H11K) (Shibata et al., 2005; Miller et al., 2008; Depre et al., 2006). Furthermore, Lee and co-workers (2009) have also suggested that the activation of AMPK by AICAR protects the kidney against ischemia and reperfusion induced injury.

The beneficial effects on the cardiovascular system are not only due to an AMPK-mediated prevention of the progression of heart failure (Sasaki et al., 2009), but also due to an improvement of the vasodilator function (Katakam et al., 2000; Sartoretto et al., 2005). Goirand et al., (2007) has shown that pharmacological activation of AMPK significantly induced relaxation in an aortic ring model. As stated above (Section 1.3), cellular contraction and relaxation, in endothelial as well as in smooth muscle cells, are

primarily controlled by MLC phosphorylation and dephosphorylation, respectively. Calcium-induced MLCK activation and Rho-kinase or PKC dependent MLCP inhibition causes elevated MLC phosphorylation which consequently promotes cellular contraction (Wysolmerski and Lagunoff, 1990; Fukata et al., 2001; Kitazawa et al., 1999) while relaxation generally depends on calcium withdrawal, calcium desensitization, MLCP activation and/or MLCK inhibition. AMPK activation could be involved in the regulation of these pathways under physiological and pathological conditions like hypoxia or ischemia. Hypoxia-induced AMPK activation (Rubin et al., 2005) may induce vasorelaxation by calcium-dependent or independent pathway (Thorne et al., 2004) through increasing the activity of MLCP by dephosphorylating MYPT1 (Wardle et al., 2006). A recent study has clearly shown an important role of AMPK in smooth muscle cell contractility (Wang et al., 2011). Activation of AMPK by AICAR significantly inhibited the agonist-induced phosphorylation of MLC and MYPT1. Moreover, AMPK inhibition potentated the agonist-induced contraction of mesenteric and aortic vessels that was associated with an increased blood pressure in mice.

The ubiquitous, protective role of AMPK in the cardiovascular system is widely recognized and pharmacological targeting of AMPK is well established as therapeutic strategy to treat patients. However, the role of AMPK in endothelial barrier, one of the fundamental functions of the endothelium, is still not fully understood. Gaskin et al. (2007) has reported that activation of AMPK reduces IR-induced leukocyte-endothelial cell interaction, indicating a protective role of AMPK in the endothelium. Recently, it has been shown that AMPK is involved in the regulation of endothelial permeability of the basal barrier function and can prevent TNF-induced hyperpermeability (Dixit et al.,

2008; Creighton et al., 2011), the underlying molecular mechanisms, however, are largely unknown.

## 1.7 Aims and objectives of the study

It is the aim of this study to analyze the mechanism by which AMPK regulates the endothelial barrier under physiological conditions and how AMPK-mediated pathway protect against reperfusoin-induced endothelial barrier failure. As mentioned above, a number of studies have examined the protective effects of AMPK activation against HR injury, however, little is known about the mechanisms involved in this protection. The present study aims to examine the protective effect of AMPK activation primarily focusing on key regulators of endothelial barrier, i.e. the endothelial junctions and contractile machinery. The molecular mechanisms of AMPK-mediated effects on barrier function will be analyzed in a model of cultured endothelial monolayers from human umbilical veins. A model of isolated saline perfused mouse hearts will be applied to prove the protective effects of AMPK on endothelial barrier in an intact coronary system.

The aims of this thesis are:

- To determine whether downregulation of AMPKα or its isoforms has functional consequence on endothelial barrier function and adhesion structures.
- To determine whether pharmacological activation of AMPK protects the endothelial barrier against reperfusion-induced failure.

- To determine whether pharmacological activation of AMPK inhibits the reperfusion-evoked morphological changes of adherens junction, actin stress fiber formation and reperfusion-induced MLC phosphorylation.
- To determine whether enhancing the AMPK activity at the onset of reperfusion confers cardioprotection in the isolated *ex vivo* mouse heart.

# 2. Materials

## 2.1 Chemicals and reagents

| | |
|---|---|
| Acrylamide | Carl Roth, Karlsruhe, Germany |
| Adenine 9-ß-d- arabinofuranoside | Sigma-Aldrich, Steinheim, Germany |
| Albumin | Sigma-Aldrich, Steinheim, Germany |
| Amino hexanoic acid | Merck, Darmstadt, Germany |
| Aminoimidazole-4-carboxamide-1-riboside | Calbiochem, San Diego, USA |
| Ammonium persulfate | SERVA, Heidelberg, Germany |
| Ammonium sulfate | Merck, Darmstadt, Germany |
| Benzonase® | Merck, Darmstadt, Germany |
| bFGF | PromoCell, Heidelberg, Germany |
| Bisacrylamide | Carl Roth, Karlsruhe, Germany |
| Bovine serum albumin | Sigma-Aldrich, Steinheim,Germany |
| Bromophenol blue | Sigma-Aldrich, Steinheim,Germany |
| Calcium chloride | Merck, Darmstadt, Germany |
| Collagenase II | PAA Labs, Pasching, Austria |
| Culture dishes | BD, Heidelberg, Germany |
| Di-sodium hydrogen phosphate | Carl Roth, Karlsruhe, Germany |
| Durapore Membrane Filter 0.45 µm diameter | MILLIPORE, Eschborn, Germany |
| EDTA | Carl Roth, Karlsruhe, Germany |
| EGTA | Boehringer, Mannheim, Germany |

| | |
|---|---|
| Endothelial cell basal medium® | PromoCell, Heidelberg, Germany |
| Endothelial cell growth supplement | PromoCell, Heidelberg, Germany |
| Eppendorf tubes (0.5, 1.5, 2 ml) | Eppendorf, Hamburg, Germany |
| Falcon tubes (50 ml, 12 ml) | BD, Heidelberg, Germany |
| FCS | PAA, Pasching, Austria |
| Filter papers | Biotech-Fischer, Reiskirchen, Germany |
| Fura-2 AM | Molecular Probes, Eugene, OR, USA |
| Gentamycin | Gibco BRL, Eggenstein, Germany |
| Glass coverslips | Menzel, Braunschweig, Germany |
| Glucose | Merck, Darmstadt, Germany |
| Glycerol (100%) | Sigma-Aldrich, Steinheim, Germany |
| Glycine | Carl Roth, Karlsruhe, Germany |
| Haparin | Ratiopharm GmbH, Ulm, Germany |
| HBSS | PAA Laboratories, Pasching, Austria |
| hEGF | PromoCell, Heidelberg, Germany |
| HEPES | Sigma-Aldrich, Steinheim, Germany |
| High molecular weight marker | Sigma-Aldrich, Steinheim, Germany |
| Jet Si$^{TM}$ ENDO | Polyplus-transfection, Strasbourg, France |
| Low molecular weight Standard | PeqLab Biotechnologie, Erlangen, Germany |
| Magnesium chloride | Fluka, Buchs, Switzerland |
| Magnesium sulfate | Merck, Darmstadt, Germany |
| β-mercaptoethanol | Merck, Darmstadt, Germany |
| Methanol | Merck, Darmstadt, Germany |
| Millipore water | Millipore, Eschborn, Germany |

| | |
|---|---|
| $N_2$ gas | Air Liquid, Krefeld, Germany |
| Nitrocellulose membrane | Schleicher and Schuell, Dassel, Germany |
| Non-fat milk powder | Applichem, Darmstadt, Germany |
| OptiMEM medium | Gibco BRL, Eggenstein, Germany |
| Penicillin/streptomycin | Gibco BRL, Eggenstein, Germany |
| Phalloidine TRITC-conjugated | Sigma, Deisenhofen, Germany |
| Pipette tips | Eppendorf, Hamburg, Germany |
| Pipettes | Eppendorf, Hamburg, Germany |
| Ponceau S solution | SERVA, Heidelberg, Germany |
| Potassium chloride | Merck, Darmstadt, Germany |
| Potassium dihydrogen phosphate | Merck, Darmstadt, Germany |
| Page rular | Fermentas, St.Leon-Rot, Germany |
| Rubber policeman | BD, Heidelberg, Germany |
| Scalpel (disposible) | Feather, Osaka, Japan |
| Sodium bicarbonate | Carl Roth, Karlsruhe, Germany |
| Sodium chloride | Carl Roth, Karlsruhe, Germany |
| Sodium di-hydrogen phosphate | Carl Roth, Karlsruhe, Germany |
| Sodium dodecyl sulfate | SERVA, Heidelberg, Germany |
| Sodium hydrogen carbonate | Merck, Darmstadt, Germany |
| Sodium hydroxide | Carl Roth, Karlsruhe, Germany |
| Sodium pyruvate | Sigma, Deisenhofen, Germany |
| Sterile filters (0.22 µm) | Sartorius, Goettingen, Germany |
| Sterile pipettes | BD, Heidelberg, Germany |
| Stripping buffer | Thermo Scientific (Pierce), Rockford, USA |

| | |
|---|---|
| Super signal-west (ECL solution) | Pierce biotech, Bonn, Germany |
| Syringes (20 ml, 2 ml) | BD, Heidelberg, Germany |
| TEMED | Sigma-Aldrich, Steinheim, Germany |
| Transwell membrane filters | Corning, NY, USA |
| Tris base | Carl Roth, Karlsruhe, Germany |
| Triton X-100 | SERVA, Heidelberg, Germany |
| Trypsin-EDTA solution | Biochrom AG, Berlin, Germany |
| Tween 20 | Amersham Biosciences, Buckinghamshire, UK |
| Urethane | Sigma-Aldrich, Steinheim, Germany |
| Whatman 3 MM filter paper | Millipore, Eschborn, Germany |

## 2.2 Antibodies

**Primary antibodies:**

| | |
|---|---|
| Anti-Actin (Mouse IgG) | Sigma, Steinheim, Germany |
| Anti-AMPKα (Rabbit IgG) | Cell Signaling Technology, Frankfurt, Germany |
| Anti-AMPKα1 (Rabbit IgG) | Cell Signaling Technology, Frankfurt, Germany |
| Anti-AMPKα2 (Rabbit IgG) | Cell Signaling Technology, Frankfurt, Germany |
| Anti-phospho AMPK Thr172 (Rabbit IgG) | Cell Signaling Technology, Frankfurt, Germany |
| Anti-MLC (Mouse IgM) | Sigma, Steinheim, Germany |
| Anti-phospho MLC (Rabbit IgG) | Cell Signaling Technology, Beverly, USA |
| Anti-phospho MYPT1 Thr850 (Rabbit IgG) | Upstate, Charlottesville, USA |
| Anti-Vinculin (Mouse IgG) | Sigma, Steinheim, Germany |

| | |
|---|---|
| Anti-VE-cadherin (Mouse IgG) | Santa Cruz Biotechnology, Heidelberg, Germany |
| Anti-β-catenin (Mouse IgG) | BD Transduction Laboratories, Heidelberg, Germany |

**Secondary antibodies:**

| | |
|---|---|
| Anti-mouse IgG HRP-conjugated | Amersham, Pharmacia, UK |
| Anti-mouse IgM HRP-conjugated | Zymed Lab, San Francisco, USA |
| Anti-rabbit IgG HRP-conjugated | Amersham Pharmacia, Freiburg, Germany |
| Anti-mouse IgG Alexa 488-conjugated | Invitrogen, Karlsruhe, Germany |
| Anti-rabbit IgG Alexa 488-conjugated | Invitrogen, Karlsruhe, Germany |

### 2.3 siRNA transfection

| | |
|---|---|
| AMPKα1/2 siRNA | Santa Cruz Biotechnology, Heidelberg, Germany |
| AMPKα1 siRNA | Santa Cruz Biotechnology, Heidelberg, Germany |
| AMPKα2 siRNA | Santa Cruz Biotechnology, Heidelberg, Germany |
| Negative control siRNA | Eurogentec, Köln, Germany. |

### 2.4 Laboratory instruments

| | |
|---|---|
| Beckman Allegra 64R centrifuge | Beckman Coulter, Fullerton, USA |
| Beckman TL 100 ultracentrifuge | Beckman Coulter, Fullerton, USA |
| Blood gas analyzer ABL5 | Radiometer GmbH, Willich, Germany |
| Electroblot chambers | Biotech-Fischer, Reiskirchen, Germany |
| Electrophoresis apparatus | Biometra, Goettingen, Germany |
| Flow sensor ME2PXN104 | beAltron Medical Electronics, Fuerstenfeldbruck, Germany |

| | |
|---|---|
| Gel documentation system (ChemiSmart 5000) | PeqLab, Erlangen, Germany |
| Glass ware | Schott, Mainz, Germany |
| Hamilton syringe | Hamilton, Bonaduz, Switzerland |
| Hypoxia chamber | Self-made at institute's workshop |
| Incubators | Heraeus, Hanau, Germany |
| Infusion pump | Precidor Infors AG, Basel, Switzerland |
| Laminar flow hood | Heraeus, Hanau, Germany |
| LSM 510 | Zeiss, Jena, Germany |
| Magnet stirrer | Jahnke und Kunkel, Staufen, Germany |
| MiniPlus 3 Peristaltic pump | Gilson, Villiers, France |
| Neubauer chamber | Superior, Marienfeld, Germany |
| Phase contrast microscope | Olympus, Japan |
| pH-Meter | WTW Weinheim, Germany |
| Photometer | Carl Zeiss, Jena, Germany |
| Power supply | Biometra, Goettingen, Germany |
| Pressure transducer 11.4123-01 | Gould Instruments Systems Inc, Gould, Statham, USA |
| Recirculation thermostat Typ B | LAUDA GMBH & CO. KG Lauda- Königshofen, Germany |
| Rocker | Biometra, Goettingen, Germany |
| Shaker | Biometra, Göttingen, Germany |
| Stereomicroscope- Zeiss Stemi 1000 | Carl Zeiss AG, Oberkochen, Germany |
| Table top (centrifuge) | Eppendorf, Hamburg, Germany |

| | |
|---|---|
| Transit time tubing flowmeter TS410 | Transonic Systems, Ithaca, USA |
| Vortexer | Heidolph, Kelheim, Germany |
| Water bath | Julabo, Seelbach, Germany |
| Water demineralization unit | Millipore, Eschborn, Germany |

## 2.5 Software

| | |
|---|---|
| Microsoft Excel 2000 | Microsoft Corp, USA |
| Microsoft Word 2000 | Microsoft Corp, USA |
| Microsoft Windows XP | Microsoft Corp, USA |
| Quantity One analysis software | Bio Rad, Hercules, USA |
| LSM 510 | Carl-Zeiss, Heidelberg, Germany |
| ChemiSmart 5000 | PeqLab biotechnologie, Erlangen, Germany |
| GraphPad Prism v5.0 software | GraphPad Software, San Diego, USA |
| PoNeMah Physiology Platform | |
| P3Plus v3.322 | Gould Inc., OH, USA |
| TillVision™ | Till Photonics™, Martinsried, Germany |

# 3. Methods

## 3.1 Cell culture

### Isolation of human umbilical vein endothelial cells

**Collagenase solution:**

| | |
|---|---|
| HBSS | x ml |
| Collagenase II, 293 IU/mg (wt/vol) | 0.025 % |
| $MgCl_2$ | 0.5 mM |
| $CaCl_2$ | 1.5 mM |

**Endothelial cell culture medium**

Endothelial cell basal medium (PromoCell®) supplemented with

| | |
|---|---|
| FCS (vol/vol) | 10 % |
| Endothelial cell growth supplement/Heparin (wt/vol) | 0.4 % |
| Hydrocortisone (wt/vol) | 0.1 % |
| Basic fibroblast factor | 1 ng/ml |
| Epidermal growth factor | 0.1 ng/ml |
| Penicillin/streptomycin (vol/vol) | 2 % |

**Procedure:** The procedure conforms to the principles outlined in the "Declaration of Helsinki" (Cardiovascular Research 1997; 35:2–4). Human umbilical vein endothelial cells (HUVEC) were isolated from freshly collected umbilical cords (University Hospital Giessen) according to Jaffe et al. (1973) with some modifications. To clean the traces of blood, umbilical veins were perfused with HBSS ($KH_2PO_4$ 0.44 mM, KCl 5.37 mM, $Na_2HPO_4$ 0.34 mM, NaCl 136.89 mM, and D-Glucose 5.55 mM) and collagenase solution was filled in lumen of the vein followed by 20-30 min incubation at 37 °C. After

incubation, collagenase solution having EC was inactivated and flushed from the umbilical veins by perfusing with 30 ml of HBSS containing 3% (vol/vol) FCS. Effluent was collected in a falcon tube and centrifuged at 250 x g at room temperature for 5 min. The supernatant was discarded and the cell pellet was resuspended in endothelial cell culture medium containing 0.1% (vol/vol) gentamycin. The cell suspension was seeded on 3-4 primary cell-culture dishes and incubated for 2 hrs at 37 ℃ with 5% $CO_2$ in a humidified environment. To remove erythrocytes, non-adherent cells and cell debris, cells were washed 2-3 times with HBSS and incubated with endothelial cell culture medium at 37° C and 5% $CO_2$. Endothelial cell culture medium was replaced with fresh medium after 24 hrs and cells were grown to confluence.

### 3.2 Sub-culturing of endothelial cell

Confluent primary EC were trypsinized in phosphate-buffered saline 5-7 days after isolation [PBS; composition in mM: 137 NaCl, 2.7 KCl, 1.7 $KH_2PO_4$, and 10 $Na_2HPO_4$; pH 7.4, supplemented with 0.05% (wt/vol) trypsin, and 0.02% (wt/vol) EDTA] and cultured in endothelial cell culture medium at a density of $5x10^4$ cells/$cm^2$. To measure the trypan blue-labeled albumin permeability across the endothelial monolayers, cells were cultured on polycarbonate Transwell® filters whereas 35 mm or 60 mm cell culture dishes were used for other experiments. For immunocytochemistry and intercellular gap formation, cells were cultured on 25mm glass coverslips. Experiments were performed with confluent endothelial monolayers of either primary or passage 1, 3 days after seeding.

### 3.3 General incubation conditions

HBSS was the basal medium used in incubations supplemented freshly with 1.3 mM $CaCl_2$ and 1.2 mM $MgCl_2$. After 30 min incubation period on heating plates at 37° C, cells were stimulated with the agents as indicated. Stock solutions of AICAR and Ara-A were prepared immediately before use with $H_2O$ and 0.1 M hydrochloric acid (HCl) respectively. Cells were stimulated with the appropriate volumes of these solutions making a final concentration of solvent less then 0.1% (vol/vol). The same final concentration of 0.1 M HCl was added in all respective control experiments. To findout the optimal effective concentration of agents to be used in the present study, concentration-response relationships were determined. The agents were applied in their optimum effective concentrations as follows: AICAR (1 mM), Ara-A (1 mM).

### 3.4 Experimental protocol for hypoxia-reperfusion

Confluent endothelial cells were incubated with HBSS supplemented freshly with 1.3 mM $CaCl_2$ and 1.2 mM $MgCl_2$ and equilibrated on heating plates at 37 °C for 30 min. Hypoxia was produced in an air tight incubation chamber (hypoxia chamber) by exposing cells to a continuous stream of 100% humidified $N_2$ gas ($Po_2 < 5$ mm Hg) for 1 hr, while the normoxic controls were exposed to humidified air ($Po_2 = 140$ mm Hg) on a heating plate at 37° C. Following 1 hr of hypoxia, cells were reperfused in HBSS supplemented with 1.3 mM $CaCl_2$ and 1.2 mM $MgCl_2$ on the heating plates at 37 °C for 45 min. To investigate the effect on cell signaling and endothelial barrier function, pharmacological activators and inhibitors were added at the onset of reperfusion.

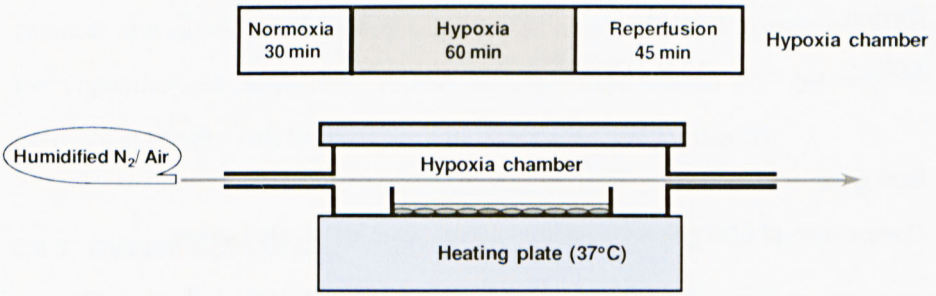


## 3.5 Protein analysis

### 3.5.1 Sample preparation

After washing with HBSS, endothelial cells were lysed in 200 µl 2x SDS sample buffer [250 mM Tris/HCl; pH 6.8, 20% (vol/vol) glycerol, 4% (wt/vol) SDS, 1% (vol/vol) mercaptoethanol, 0.001% (wt/vol) bromphenol blue, and 10 mM DTT (added freshly before use)]. Total cell lysate was scraped with help of a rubber policeman and collected in an Eppendorf tube after adding 50 IU/ml Benzonase and 2 mM $MgCl_2$. Samples were immediately used after denaturation at 95 °C for 5 min or stored at –20 °C for future use.

### 3.5.2 SDS-polyacrylamide gel electrophoresis (SDS-PAGE)

| | | |
|---|---|---|
| Resolving gel buffer: | Tris/HCl; pH 8.8 | 120 mM |
| Stacking gel buffer: | Tris/HCl; pH 6.8 | 120 mM |

**10x Gel running buffer**

| | |
|---|---|
| Tris | 250 mM |
| Glycine | 2.0 M |
| SDS | 10 % (wt/vol) |

**SDS gels**

Composition of SDS gels with different percentages is indicated below:

| Gels | Resolving gels | | | | Stacking gel |
|---|---|---|---|---|---|
| Solutions | 7.5 % | 10 % | 12.5 % | 15 % | 6 % |
| Acryamide 40% (wt/vol) | 7 ml | 10.2 ml | 12.7 ml | 15.3 ml | 3.8 ml |
| Bisacrylamide 2% (wt/vol) | 4.2 ml | 5.6 ml | 7.0 ml | 8.4 ml | 2.0 ml |
| Millipore water | 17.7 ml | 13.8 ml | 9.8 ml | 5.8 ml | 17.5 ml |
| Resolving gel buffer | 9.5 ml | 9.5 ml | 9.5 ml | 9.5 ml | ------ |
| Stacking gel buffer | ------ | ------ | ------ | ------ | 6.0 ml |
| SDS 10% (wt/vol) | 0.4 ml | 0.4 ml | 0.4 ml | 0.4 ml | 0.25 ml |
| TEMED | 30 µl | 30 µl | 30 µl | 30 µl | 20 µl |
| APS 10% (wt/vol) | 0.4 ml | 0.4 ml | 0.4 ml | 0.4 ml | 0.25 ml |

**Procedure:** Glass plates and spacers were cleaned with water and ethanol, the resolving gel solution was poured between the glass plates after assembling the gel apparatus. The gel was layered with water-saturated butanol to prevent the oxygen getting in as this inhibits the polymerization of gel. Butanol was discarded after 3-4 hrs and top of the gel was completely rinsed with distilled water once gel was solidified. Stacking gel solution was poured on top of the resolving gel, comb was inserted

immediately and let to polymerize at room temperature for 1 hr. After stacking gel polymerization, comb was removed gently, 1x gel running buffer was added to gel chamber and sample wells were rinsed with same buffer using a syringe to romove the unpolymerized acrylamide. Protein samples were loaded and gel was run overnight at 45 volts until the bromophenol blue moved out from the gel.

### 3.5.3 Western blot analysis

Proteins from SDS-PAGE gel were transferred onto nitrocellulose membrane by a semi-dry blotting method as discribed below.

**Materials and solutions**

- Nitrocellulose membrane
- Whatman 3 MM filter paper
- Blotting chamber
- Blotting buffer (25 mM Tris HCl; 150 mM Glycine, pH 8.3; 10% (vol/vol) methanol)
- Millipore water

**Procedure:** The graphite blotting chamber was assembled in the following order; Three sheets of filter paper (Whatman® 3MM) were cut to equal sizes as the gel; thoroughly soaked in blotting buffer and placed on graphite anode blotting chamber. A nitrocellulose membrane, already equilibrated in blotting buffer was layed on top of these filter papers. Gel was placed carefully on the nitrocellulose membrane after a brief equilibration with blotting buffer and air bubbles were gently removed by rolling a

glass rod over the gel. Afterwards three sheets of filter paper, presoaked in blotting buffer were placed on the gel followed by graphite cathode blotting chamber and proteins were transferred at 0.8-0.9 mA/cm$^2$ current for approximately 2 hrs.

### 3.5.4 Ponceau staining of transferred proteins

To see whether proteins were transferred from gel, nitrocellulose membrane was stained with ponceau-S. Ponceau-S produces pink bands on the membrane with a light background, which is reversible. After washing with distilled water for 1 min the membrane was incubated for 2-3 min in ponceau-S solution with constant shaking at room temperature. After ponceau-S staining the membrane was washed with distilled water to the required contrast and photograph was taken. Subsequently the membrane was washed with 1x TBST buffer for complete destaining.

### 3.5.5 Immunodetection of proteins

**Solutions:**

10x Tris-buffered saline (TBS): 100 mM Tris/HCl (pH 7.4), 1.6 M NaCl

TBS Tween (TBST): 1x TBS, 0.1% (vol/vol) Tween 20

Blocking-buffer: BSA 4% (wt/vol) in 1x TBST or 5% (wt/vol) non-fat dried milk powder in 1x TBST

**Primary Antibodies**

| **Antibody** | **Dilution** | **Dilution buffer** |
|---|---|---|
| Anti-Actin (Mouse IgG) | 1:1000 | BSA |
| Anti-AMPK α (Rabbit IgG) | 1:1000 | Milk |

| | | |
|---|---|---|
| Anti-AMPK α1 (Rabbit IgG) | 1:1000 | Milk |
| Anti-AMPK α2 (Rabbit IgG) | 1:1000 | Milk |
| Anti-phospho AMPK Thr172 (Rabbit IgG) | 1:2000 | BSA |
| Anti-MLC (Mouse IgM) | 1:2000 | Milk |
| Anti-phospho MLC (Rabbit IgG) | 1:1000 | Milk |
| Anti-phospho MYPT1 Thr850 (Rabbit IgG) | 1:1000 | BSA |
| Anti-Vinculin (Mouse IgG) | 1:2000 | BSA |

**Secondary antibodies, horseradish peroxidase (HRP)-labeled**

| **Antibody** | **Dilution** | **Dilution buffer** |
|---|---|---|
| Anti-rabbit IgG | 1:2000 | BSA |
| Anti-mouse IgG | 1:2000 | BSA |
| Anti-mouse IgM | 1:2000 | BSA |

**Procedure:** After washing with Millipore water and 1x TBST, membrane was blocked with 1x TBST containing either 5% (wt/vol) non-fat milk powder or 4% (wt/vol) BSA at room temperature for 1 hr. After blocking, the membrane was incubated with primary antibody with gentle shaking overnight at 4 ℃. The membrane was washed 3 times for 10 min each with 1x TBST and incubated in secondary antibody for 1 hr at room temperature. The membrane was incubated with enhanced chemiluminescence (ECL) solution for 1 min after 2-3 times washing as stated before. The luminescence was detected and recorded with PeqLab, ChemiSmart gel documentation system according to manufacturer's instructions.

### 3.5.7 Stripping and reprobing of the nitrocellulose membrane

Following Western blot analysis the first set of antibodies was striped off to detect the other proteins on the same membrane by using a second set of specific antibodies. Bound antibodies were removed by washing membrane 2-3 times for 10 min each in 1x TBST. Immediately after washing, the wet membrane was incubated for 20 min at room temperature in stripping buffer with constant agitation. The membrane was then thoroughly washed 2-3 times for 10 min each in 1x TBST, blocked and reprobed with an appropriate antibody.

## 3.6 siRNA transfection of endothelial cells

To reduce the level of endogenous AMPK α protein or its isoforms, endothelial cell monolayers were transfected with small interfering RNA (siRNA) targeting against AMPK α1 and AMPK α2 (AMPK α1/2 siRNA) or either AMPK α1 (AMPK α1 siRNA) or AMPK α2 (AMPK α2 siRNA). Pre-designed siRNAs duplexes targeting against AMPK α1/2 and its both isoforms were commercially obtained from Santa Cruz Biotechnology. A scrambled nonsilencing siRNA from Eurogentec, which has no homology to any known mammalian gene, was used as a negative control (Neg siRNA). Endothelial cell monolayers were transfected at 70–80% confluency with 25 nM siRNAs using jetSI$^{TM}$-ENDO transfection reagent in serum and antibiotic free optiMEM medium according to the manufacturer's instructions. Endothelial cell culture medium containing 10% (vol/vol) FCS was added without removing the transfection mixture. Transfection medium was replaced with the endothelial cell culture medium after 24 hrs and respective experiments were performed 24 hrs after the addition of fresh medium. Protein levels were determined by Western blot analysis using specific antibodies.

### 3.7 Measurement of endothelial monolayer permeability

The permeability across the endothelial monolayer was measured in two-compartment system as described by Noll et al., (1999). The upper (luminal) and lower (abluminal) compartment was separated by a filter membrane with a pore size of 0.4μm. The EC were cultured in luminal compartment on the filter membrane and grown to fully confluent. HBSS [composition in mM: 1.3 $CaCl_2$, 1.2 $MgCl_2$, and 2% (vol/vol) fetal calf serum (FCS)] was used as a basal medium. The luminal compartment contained 2.5 ml of basal medium while 9.5 ml was added to abluminal compartment that was constantly mixed using magnetic stirrers. The luminal and abluminal compartments showed no hydrostatic pressure. Trypan blue–labeled albumin (60 μM) was added to the luminal compartment and its transfer across the endothelial monolayer was continuously monitored in the abluminal compartment by a spectrophotometer after every min. Two-wavelength measurement mode was used (trypan blue 600 nm versus control 720 nm) to prevent the measurement artifacts.

The albumin flux (F, expressed as mol/[s × $cm^2$]) across monolayer of endothelial cells with the surface (S) was measured from the increase of the albumin concentration ($d[A]_2$) during the time interval (dt) in the abluminal compartment (volume V) as shown below:

$$F = \frac{d[A]_2 / dt \times V}{S} \qquad (1)$$

The combined permeability coefficient denoted as P (cm/sec) of both endothelial monolayer and filter membrane was calculated by Fick's law of diffusion as follows:

$$P = \frac{F}{([A]_1 - [A]_2)} \qquad (2)$$

Where $[A]_1$ is concentration of albumin in luminal compartment and $[A]_2$ represents the abluminal albumin.

### 3.8 Interendothelial gap formation

Gap formation between adjacent endothelial cells was determined by planimetric analysis based on fluorescence images obtained from endothelial monolayers loaded with the fluorescent calcium indicator fura-2, using a TILL Photonics imaging system (Martinsried, Germany). For loading the cells with fura-2, endothelial monolayers cultured on glass coverslips were incubated in medium 199 plus 4% FCS containing acetoxymethyl ester of fura-2 (2.5 µM), the cell membrane permeable form of fura-2, for 60 min, followed by incubation in fura-2-free medium for 30 min. Afterwards the coverslips were transferred into a gastight incubation chamber mounted on a temperature-controlled stage (37 °C) of an inverted microscope (Olympus IX70, Hamburg, Germany). To maintain normoxic conditions, the incubation chamber (1 ml filling volume) was constantly perfused with modified HEPES buffer ($Po_2$ = 140 mm Hg; composition in mM: 140 NaCl, 2.6 KCl, 1.2 $KHPO_4$, 1.2 $MgSO_4$, 1.3 $CaCl_2$, 2.5 glucose and 25 HEPES) at a flow rate of 0.5 ml/min. The hypoxic medium did not contain glucose and equilibrated with 100% $N_2$ before and during experiments. The $Po_2$ of hypoxic medium was <1 mm Hg as determined by a polarographic oxygen sensor. The medium was pumped into the perfusion chamber through gas-tight steel capillaries. EC were exposed to 40 min hypoxia followed by 30 min reperfusion with normoxic medium. AICAR (1 mM) was added at the onset of reperfusion and administrated for the whole reperfusion period. Transfection was

performed with either 25nM AMPK siRNA α1/2 or with a negative control siRNA 48 hrs before the experiments.

To quantify the formation of gaps between adjacent EC, fluorescence images (frame: 640 x 480 pixel, width/hight) were taken every 6 seconds (excitation wavelength at 360 nm, emission wavelength at 510 nm). Afterwards, the digital fluorescence imaging were binarized by an algorithem embedded in the imaging program (TillVision™, Till Photonics™, Martinsried, Germany) which allocates the cell-free, non-fluorescent areas of the images to 0 (gaps) and the fluorescence signal of the fura-2 loaded cells to 1. Finally, the number of pixels allocated to zero was determined for each frame. The number of zero pixels determined after the hypoxic period was set to 100% gap formation, and changes of that number during reperfusion are given relative to this scale.

### 3.9 Immunofluorescence

**Solutions and materials:**

Blocking-buffer: 5% (wt/vol) BSA and 5% (vol/vol) FCS in 1x PBS

**Primary antibodies**

| **Antibody** | **Dilution** | **Dilution buffer** |
|---|---|---|
| Anti-AMPKα 1 (Rabbit IgG) | 1:200 | blocking buffer |
| Anti-AMPKα 2 (Rabbit IgG) | 1:200 | blocking buffer |
| Anti-VE-cadherin (Mouce IgG) | 1:200 | blocking buffer |
| Anti-catenin-beta (Mouse IgG) | 1:200 | blocking buffer |

**Secondary antibodies**

| Antibody | Dilution | Dilution buffer |
|---|---|---|
| Anti-mouse IgG Alexa fluor 488 | 1:200 | blocking buffer |
| Anti-rabbit IgG Alexa fluor 488 | 1:200 | blocking buffer |

**Protocol:** Confluent endothelial monolayers grown on glass coverslips were washed twice with 1x PBS, fixed with ice cold 100% methanol for 20 min at -20 ℃ or 4% (wt/vol) paraformaldehyde for 20 min at room temperature. Coverslips were washed 2-3 times for 10 min each with 1x PBS and permeabilized with 0.2% (vol/vol) Triton X-100 for 20 min. The coverslips were washed 2-3 times with 1x PBS, incubated with blocking buffer for 1 hr and probed with respective primary antibody overnight at 4 ℃. Subsequently, the coverslips were washed 2-3 times for 10 min each with 1x PBS and incubated with secondary antibodies tagged with Alexa fluor 488 for 1 hr at room temperature. To stain the actin stress fibers, EC were treated with TRITC-labeled phalloidin (1:50) for 1 hr after blocking. Coverslips were gently washed with 1x PBS 2-3 times for 10 min each and finally embedded in a drop of 40% glycerol/PBS solution (pH 8.5) on glass slides. Confocal images were taken using laser scanning microscopy.

### 3.10 Myocardial water content determination

All experiments were performed in accordance with the recommendations in the Guide for the Care and Use of Laboratory Animals of the German law of animal welfare. The procedure was approved by the Landesdirektion Sachsen, Germany (§6. Abs. 1 Satz 2 Nr. 4 Tierschutzgesetz; permit number 27-9168.24-1). Hearts from male 8 to 10 week-old C57BL6 mice, with an average weight of 20–25 g, were excised rapidly,

immersed in ice-cold buffer and mounted on a Langendorff perfusion system via the aorta on a perfusion cannula. Hearts were then perfused with Krebs-Henseleit buffer containing (composition in mM): NaCl 116, KCl 4.6, $MgSO_4$ 1.2, $KH_2PO_4$ 1.2, $NaHCO_3$ 24.8, $CaCl_2$ 3.0, glucose 8.3, pyruvate 2, and EDTA-Na 0.5, at constant pressure for a brief equilibration period (20 min), which preceded every experiment. The buffer was filterated with 0.45 µm diameter Durapore membrane filter, whose pH was maintained at 7.38-7.5 by gassing with corbogen (95% $O_2$ and 5% $CO_2$). The thermostatic heart chamber was flushed with humidified air during normoxia. During ischemia (no-flow), it was flushed with a humidified 95% $N_2$ and 5% $CO_2$ gas mixture. After 60 min of no-flow ischemia, hearts were again resupplied with oxygen by reperfusion of a Krebs-Henseleit buffer for 40 min. Constant flow was selected for the reperfusion of ischemic hearts. To perform the heart perfusion on optimum and defined conditions, the following parameters were thoroughly monitored throughout the whole perfusion period. Total coronary flow was measured using an ultrasonic transit-time flow meter inserted in the arterial perfusion line. Left ventricular pressure (LVP) was assessed isovolumically using a self-constructed fluid-filled latex balloon advanced into the ventricle via the left atrium and connected to a pressure transducer. Coronary perfusion pressure was measured through a pressure transducer connected to the perfusion cannula. Heart rate was calculated electronically from the LVP recording. Measurements of coronary perfusion pressure, coronary flow, LVP, and heart rate were analog to digital (A/D) converted and acquired (data sampling rate 100 Hz), displayed, and stored on a computer. The data were processed using PoNeMah Physiology Platform P3Plus v3.322.

AICAR (0.5 mM) was dissolved in Krebs-Henseleit buffer and administered at the onset of reperfusion using an infusion pump. At the end of each experiment wet weight and after 48 hrs of freeze drying at -45° C dry weight of the mouse hearts were measured.

### 3.11 Statistical analysis

Statistical analysis was performed using GraphPad Prism 5 software. Data are given as means ±SD of 3-5 experiments using independent cell preparations. For comparison of means between groups the one-way analysis of variance (one-way ANOVA) was used followed by a Student-Newman-Keuls post hoc test. Probability (P) values of less than 0.05 were considered significant ($P < 0.05$).

# 4. Results

## 4.1 siRNA-mediated reduction of AMPKα1/2 protein in endothelial cells

To investigate the potential role of AMPK in endothelial barrier function, a siRNA approach was used to reduce the cellular contents of the catalytic AMPKα protein. Endothelial monolayers were transfected with siRNA duplexes targeted to human AMPKα1 and α2 (AMPKα1/2 siRNA) or a nonspecific negative control siRNA (Neg siRNA). The AMPK α has at least two isoforms (α1 and α2) so transfection of EC with AMPK α1/2-targeted siRNA efficiently reduced the protein levels of both isoforms (48 hours after transfection), as demonstrated by immunoblots of total cell lysates (Fig. 4.1A). Densitometric analysis (Fig. 4.1B) shows that transfection with 25 nM AMPK α1/2 siRNA resulted in a significant reduction of AMPK α1 and AMPK α2 protein contents in comparison to negative control siRNA or non-transfected cells. Under all experimental conditions, levels of vinculin protein in cell lysates remained unaffected by transfection with either AMPK α1/2 or negative control siRNA. For all further experiments, endothelial monolayers were transfected with same concentartions of AMPKα1/2 siRNA for 48 hrs.

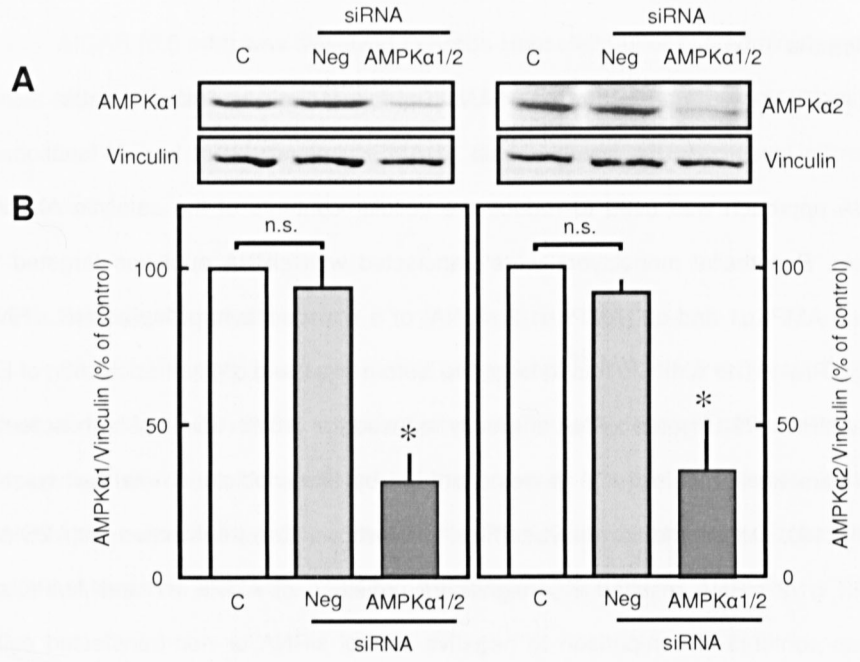


**Fig. 4.1** Effect of siRNA-mediated reduction of AMPKα1/2 protein in endothelial cells. Cultured endothelial monolayers were left non-transfected or were transfected with 25 nM siRNA targeted against AMPKα1/2 or negative control siRNA (Neg siRNA). After 48 hrs cells were lysed and levels of AMPKα1, AMPKα2 and vinculin were assessed by immunoblotting. Non-transfected cells served as a control (C). **A)** Representative Western blots of total cell lysates using anti-AMPKα1, anti-AMPKα2 and anti-vinculin antibody. Left panel shows representative Western blot of AMPKα1 and right panel ofAMPKα2. **B)** Densitometric analysis of Western blots assessed for AMPKα1 (left), AMPKα2 (right) and vinculin. The ratio of AMPKα1 and AMPKα2 to vinculin in non-transfected control cells was set to 100 %. Data are means ± SD of 3-4 separate

experiments with independent cell preparations. *P < 0.05 vs. Neg siRNA; n.s., not significant different.

### 4.2 siRNA-mediated reduction of AMPKα1/2 protein results in increased basal endothelial permeability

Previous studies have shown that overexpression of dominant negative AMPK mutant was associated with a failure of endothelial barrier function (Dixit et al., 2008). Here we studied the effect of siRNA-mediated AMPKα1/2 protein reduction on basal endothelial permeability and possible mechanism behind this process by a direct molecular approach using siRNA. As shown in Fig. 4.2, loss of AMPKα1/2 protein contents resulted in a significant increase in basal permeability compared to endothelial monolayers treated with negative control siRNA, demonstrating that reduction of the AMPKα1 and α2 content impairs endothelial barrier function.

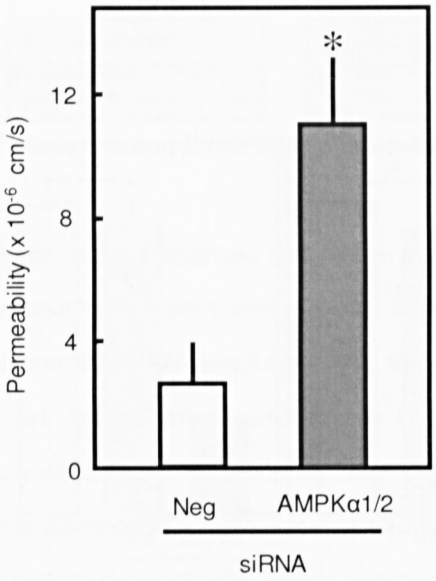


**Fig. 4.2** Effect of siRNA-mediated reduction of cellular AMPKα1/2 protein on basal endothelial permeability. Cultured endothelial monolayers were transfected with 25 nM siRNA targeted against AMPKα1/2 or with negative control siRNA (Neg siRNA). Permeability of trypan blue-labeled albumin across endothelial monolayers is depicted after 140 min under basal conditions. AMPKα1/2 siRNA transfected cells were compared to negative control siRNA treated cells. The albumin permeability in AMPKα1/2 siRNA treated monolayers is significantly different from the negative control siRNA treated monolayers. Data are means ±SD of 3-4 separate experiments with independent cell preparations. * $P < 0.05$ vs. Neg siRNA.

### 4.3 siRNA-mediated reduction of AMPK1/2 protein causes disturbance of endothelial junctions and induces F-actin stress fiber formation

To further characterize the effect of AMPKα1/2 on distribution of endothelial junction proteins and cytoskeleton, immunofluorescence analysis of both AMPKα isoforms was performed in non-transfected EC or cells transfected with AMPKα1/2 or negative control siRNA. It can be seen from Fig. 4.3 that the AMPKα1 is mainly detected in the cytoplasm while AMPKα2 is found in the cytoplasm as well as in the nucleus of the cells. Consistent with the Western blot results (Fig. 4.1), immunofluorescence also revealed that cells transfected with AMPKα1/2 siRNA showed a marked reduction of AMPKα1 and AMPKα2 levels compared with non-transfected cells or cells transfected with negative control siRNA.

The association of adherens junction proteins is required for full cellular control of endothelial permeability and junctional stability. We next analyzed whether reduction of AMPKα1/2 content would affect the morphology of adherens junctions and actin cytoskeleton in EC. Fig. 4.3 shows that VE-cadherin and β-catenin was nicely decorated at the cell boarders of both non-transfected cells and cells transfected with negative control siRNA. Reduction of AMPKα1/2 content caused disintegration of the VE-cadherin/β-catenin-mediated cell adhesion structures and led to gap formation between adjacent cells. To investigate whether reduction of AMPKα1/2 content affects actin cytoskeleton in EC, AMPKα1/2 siRNA-transfected cells were stained using TRITC-labeled phalloidin. The microscopic analysis has shown (Fig. 4.3) that siRNA-mediated reduction of AMPKα1/2 evoked a strong reorganization the F-actin cytoskeleton characterized by an increase in actin stress fibers. In contrast, in control cells actin was

concentrated along the cellular borders, as so called cortical actin, and was generally absent in the central regions.

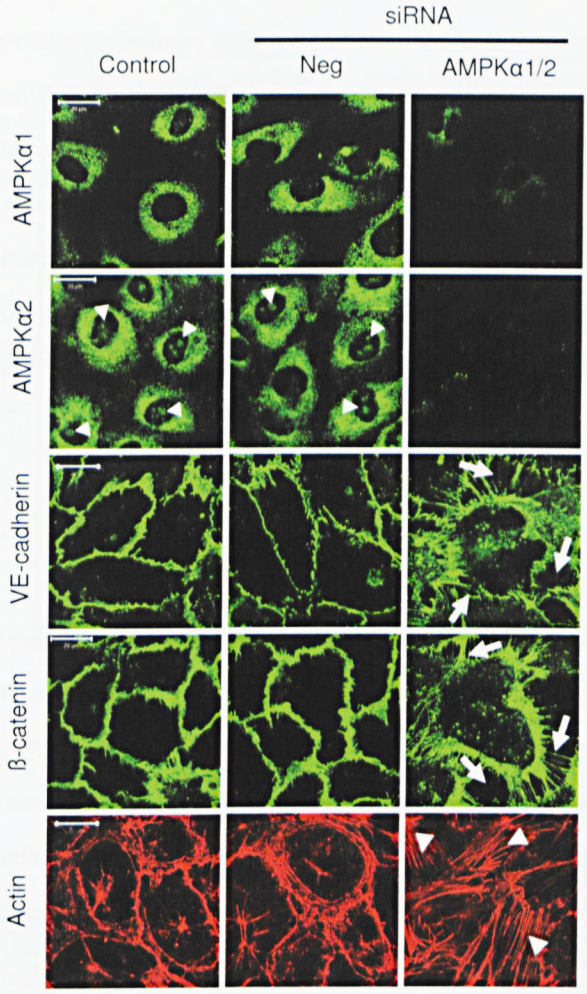


**Fig. 4.3** Effect of siRNA-mediated reduction of cellular AMPK α1/2 protein on the distribution of AMPKα1, AMPKα2, endothelial junctional protein and actin cytoskeleton. Cultured endothelial monolyers were left non-transfected (control) or were transfected with 25 nM siRNA targeted against AMPKα1/2 or negative control siRNA (Neg siRNA).

Immunocytochemistry and confocal fluorescence microscopy were performed 48 hrs after transfection to analyze of changes in localization of AMPKα1, AMPKα2, and morphological changes of VE-cadherin, β-catenin, and actin. AMPKα1 is mainly detected in the cytoplasm while AMPKα2 is found in the cytoplasm as well as in the nucleus (arrowheads) of the cells. Changes in localization of VE-cadherin and β-catenin show that gaps are formed between adjacent cells (arrows). Arrowheads denote formation of F-actin stress fibers. One representative image of three independent experiments is shown. Bar = 20 μm.

### 4.4 siRNA-mediated reduction of the α1- or α2 AMPK isoform results in increased endothelial permeability

To make a more specific evaluation of the AMPKα isoforms involved in the regulation of endothelial barrier function, EC were transfected with siRNAs specifically targeting either AMPKα1 or AMPKα2. As shown in Fig. 4.4, AMPKα isoform-specific siRNA selectively reduced the protein content of its specific isoforms with no effect on the expression levels of other isoform. Trypan blue-labeled albumin permeability across confluent AMPKα1 or AMPKα2 depleted endothelial monolayers was then determined in comparison to cells treated with negative control siRNA. Interestingly, AMPKα1- or AMPKα2 protein reduction by siRNA also markedly increased the basal endothelial permeability across endothelial monolayers compared to negative siRNA treated cells (Fig. 4.4 D).

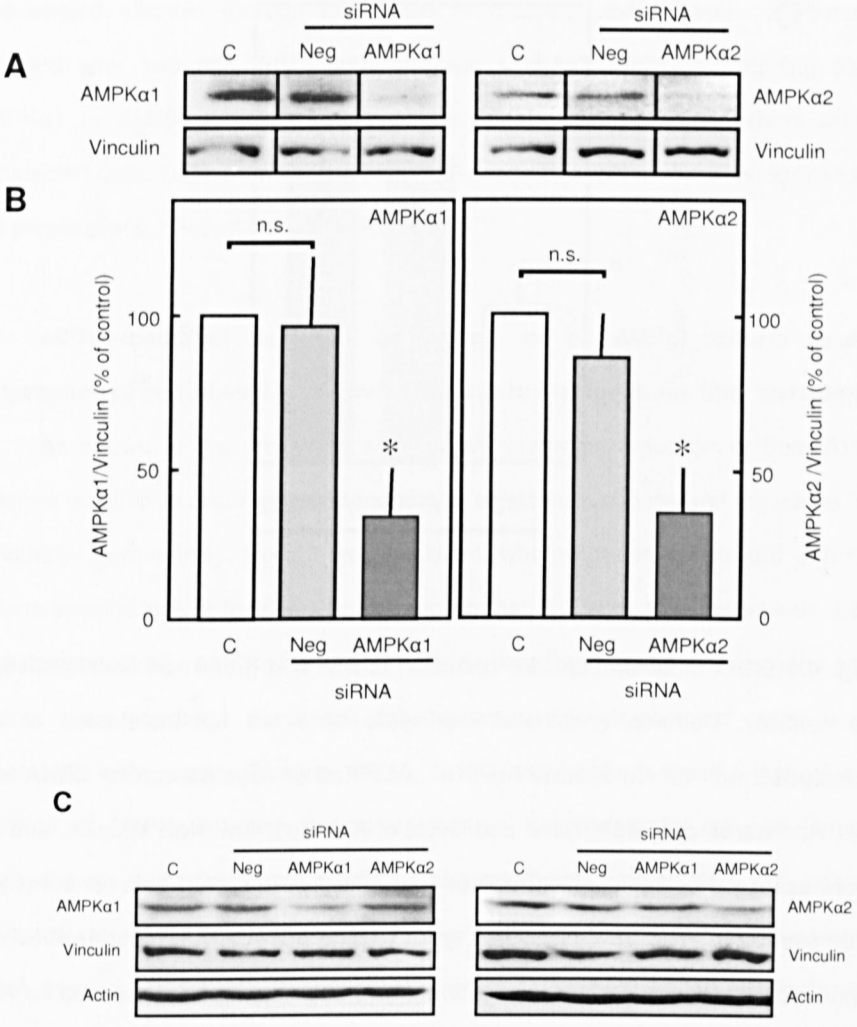
A
siRNA
C
Neg
AMPKα1
AMPKα1
Vinculin
siRNA
C
Neg
AMPKα2
AMPKα2
Vinculin
B
AMPKα1
n.s.
*
AMPKα1/Vinculin (% of control)
100
50
0
C
Neg
AMPKα1
siRNA
AMPKα2
n.s.
*
AMPKα2 /Vinculin (% of control)
100
50
0
C
Neg
AMPKα2
siRNA
C
siRNA
C
Neg
AMPKα1
AMPKα2
AMPKα1
Vinculin
Actin
siRNA
C
Neg
AMPKα1
AMPKα2
AMPKα2
Vinculin
Actin

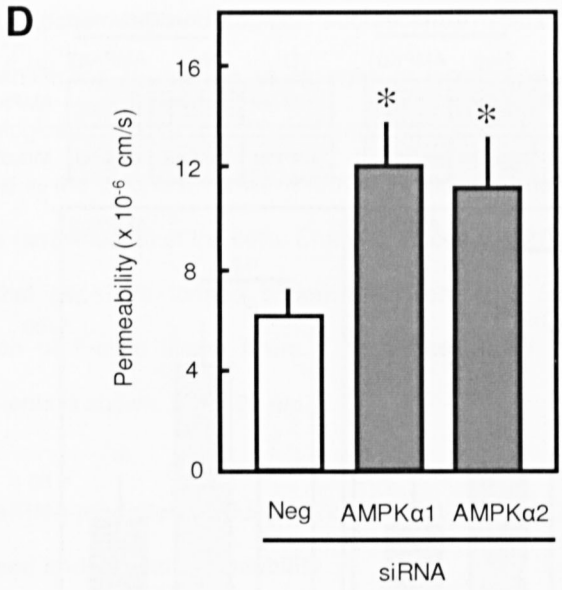


**Fig. 4.4** Effect of isoform-specific reduction of AMPK α protein on basal endothelial permeability. Cultured endothelial monolyers were left non-transfected or were transfected with 25 nM specific AMPKα1, AMPKα2 or negative control siRNA for 48 hrs. Afterwards cells were lysed and levels of AMPKα1, AMPKα2, vinculin, and actin were assessed by immunoblotting. Non-transfected cells served as a control (C). **A)** Representative Western blots of cell lysates using anti-AMPKα1, anti-AMPKα2, and anti-vinculin antibody. **B)** Densitometric analysis of Western blots assessed for AMPK α1 (left), AMPKα2 (right) and vinculin. The ratio of AMPK α1 and AMPK α2 to vinculin in non-transfected control cells was set to 100 %. Data are means ± SD of 3-4 separate experiments with independent cell preparations. * $P < 0.05$ vs. Neg siRNA; n.s., not significant. **C)** Representative Western blots of EC lysates using anti-AMPKα1, anti-AMPKα2, anti-vinculin and anti-actin antibody. **D)** Permeability of trypan

*blue-labeled albumin through endothelial monolayers under basal conditions* is depicted after 140 min. EC transfected with siRNAs specifically targeting either AMPKα1 or AMPKα2 were compared with negative control siRNA (Neg siRNA) *transfected cells. Data are means* ± SD of 2-3 separate experiments with independent cell preparations. *P<0.05 vs. Neg siRNA.

### 4.5 siRNA-mediated reduction of the α1- or α2 AMPK isoform causes disturbance of endothelial junctions and induces F-actin stress fiber formation

As shown in the preceding sections simultaneous reduction of both AMPKα isoforms resulted in disturbance of endothelial adherens junctions and increased basal endothelial permeability. Here it was analyzed, whether these effects are due to an isoform-specific loss of function. To accomplish that, EC were transfected with siRNAs targeting specifically AMPKα1 and AMPKα2. As shown in Fig. 4.5, VE-cadherin and β-catenin were localized along cell–cell borders in non-transfected cells or cells transfected with negative control siRNA. In contrast, isoform-specific loss of either AMPKα1 or AMPKα2 protein expression induced interendothelial cell gap formation resulted from the disintegration of VE-cadherin/β-catenin-mediated cell adhesion structures. Moreover, non-transfected cells or cells transfected with negative control siRNA showed cortical actin filaments that were predominant along the cell border while reduction of either α1 or α2 isoform of AMPK resulted in increased F-actin stress fiber formation.

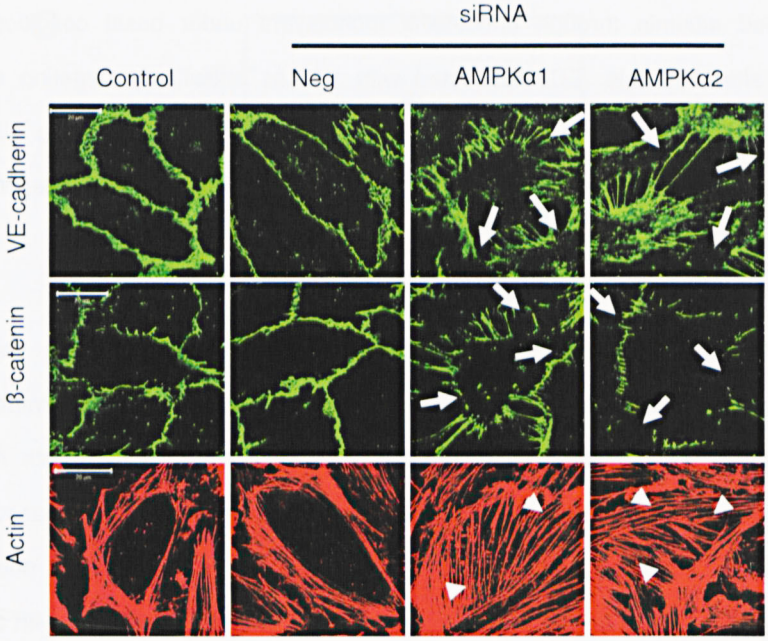


**Fig. 4.5** Effect of isoform-specific reduction of AMPK α protein on endothelial junctional protein and actin cytoskeleton. Endothelial monolayers were left non-transfected (control) or were transfected with 25 nM siRNA against AMPKα1, AMPKα2 or negative control siRNA (Neg siRNA). Immunocytochemistry and confocal fluorescence were performed 48 hrs after transfection to analyze morphological changes of VE-cadherin, β-catenin and actin. Arrowheads denote F-actin stress fibers and arrows denote gaps between the cells. One representative image of 3 independent experiments is shown. Bar = 20 μm.

## 4.6 Hypoxia-reperfusion regulates AMPK phosphorylation in endothelial cells

To test the activation state of AMPK and its association with reperfusion-induced endothelial barrier dysfunction, cells were incubated for 1 hr under hypoxic conditions followed by reperfusion for different periods of time. Normoxic cells served as control. Treated cells were lysed and analyzed for AMPK phosphorylation by Western blot. AMPK phosphorylation was estimated under normoxia (N), hypoxia (H) and reperfusion (R) using a specific antibody against the threonine 172 (Thr 172) phosphorylation site of AMPK, which has been established to be essential for its activity (Lage et al., 2008). As shown in Fig. 4.6 that AMPK phosphorylation was significantly increased in response to hypoxia. However, it already had declined below the normoxic level after 15 min and remained on that level throughout to ongoing reperfusion period.

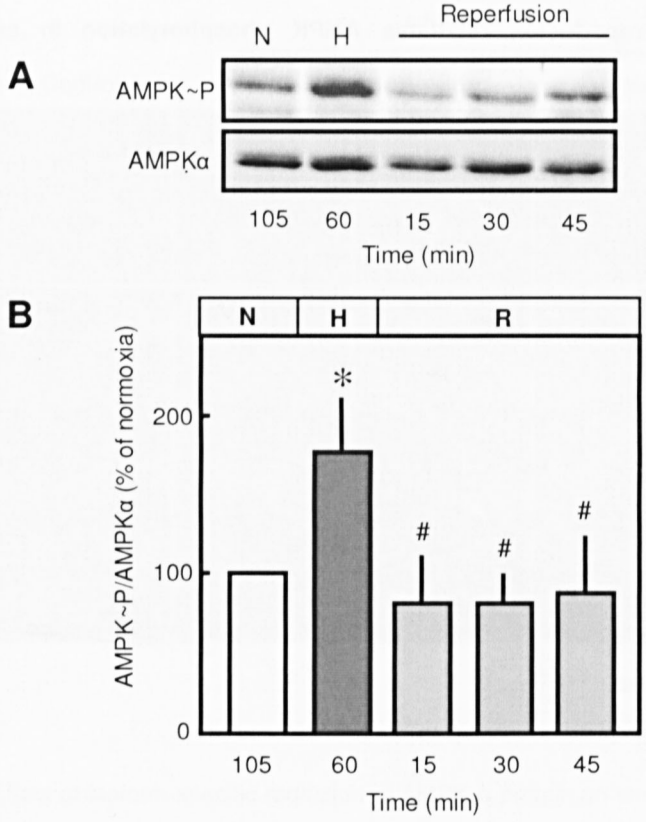


**Fig. 4.6** Effect of hypoxia-reperfusion on AMPK phosphorylation in endothelial cells. Cultured endothelial monolayers were incubated under normoxia (N; $Po_2$ = 140 mmHg; pH 7.4), hypoxia (H; $Po_2$< 5 mmHg; pH 7.4) followed by reperfusion (R; $Po_2$ = 140 mmHg; pH 7.4) for different periods of times as indicated. **A)** Representative Western blots with an anti-phospho-Thr172 AMPK antibody. **B)** Densitometric analysis of Western blots. AMPK phosphorylation relative to total AMPK α is given as % of normoxia. The ratio of normoxic control cells was set to 100%. Data are means ± SD

of 4-5 separate experiments with independent cell preparation. *P < 0.05 vs. N; #P < 0.05 vs. H.

### 4.7 AICAR increases AMPK phosphorylation in endothelial cells

In order to analyze the effect of AMPK activation on the barrier properties of endothelial monolayers, EC were incubated in presence of different concentrations of AMPK activator, AICAR (0.5, 1, and 2 mM) for 30 min at room temperature. AMPK phosphorylation was determined by Western blot analysis using phospho-AMPK antibody. As shown in Fig. 4.7, phosphorylation of AMPK at Thr172 increased in concentration-dependent manner with a maximum at 1 mM AICAR. At this concentration the increase in AMPK phosphorylation reached it maximum at 30 min. All further experiments were performed at that concentration.

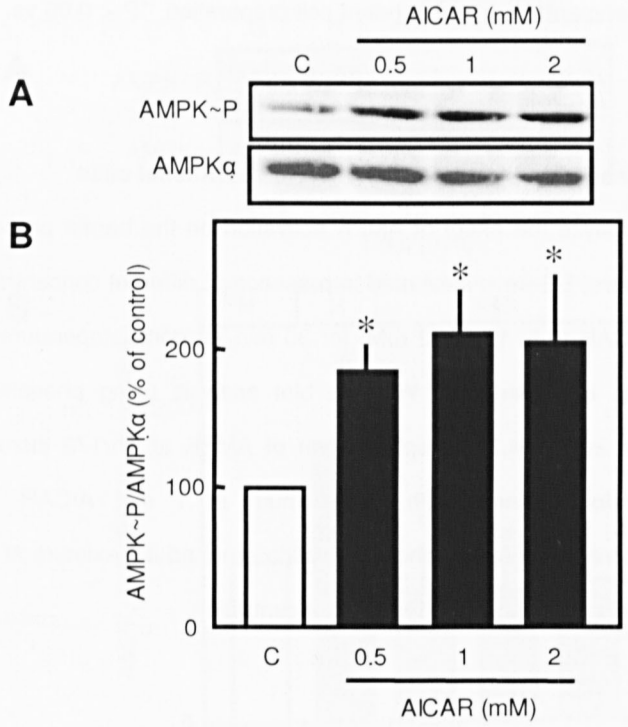


**Fig. 4.7** Effect of AICAR on AMPK phosphorylation at Thr172 in endothelial cells under basal conditions. Cultured endothelial monolayers were exposed to AICAR for 30 min at room temperature. **A)** Representative Western blots with an anti-phospho-Thr172 AMPK or anti-total AMPKα antibody. **B)** Densitometric analysis of Western blots. AMPK phosphorylation relative to total AMPKα is given as % increase compared to control (C). The ratio of control was set to 100%. Data are means ± SD of 3-4 separate experiments of independent cell preparations. * $P < 0.05$ vs. C.

### 4.8 Ara-A inhibits AMPK phosphorylation in endothelial cells

To analyze the effect of the AMPK inhibitor Ara-A on basal AMPK phosphorylation, confluent EC were exposed to increasing concentrations of Ara-A (0.5, 1, and 2 mM) at room temperature for 30 min. AMPK phosphorylation was determined by Western blot analysis using phospho-AMPK antibody. As shown in Fig. 4.8, Ara-A inhibited the AMPK phosphorylation in a concentration dependent manner. Since 1 mM of Ara-A caused an optimal dephosphorylation of AMPK at 30 min, all following incubations were done under this condition.

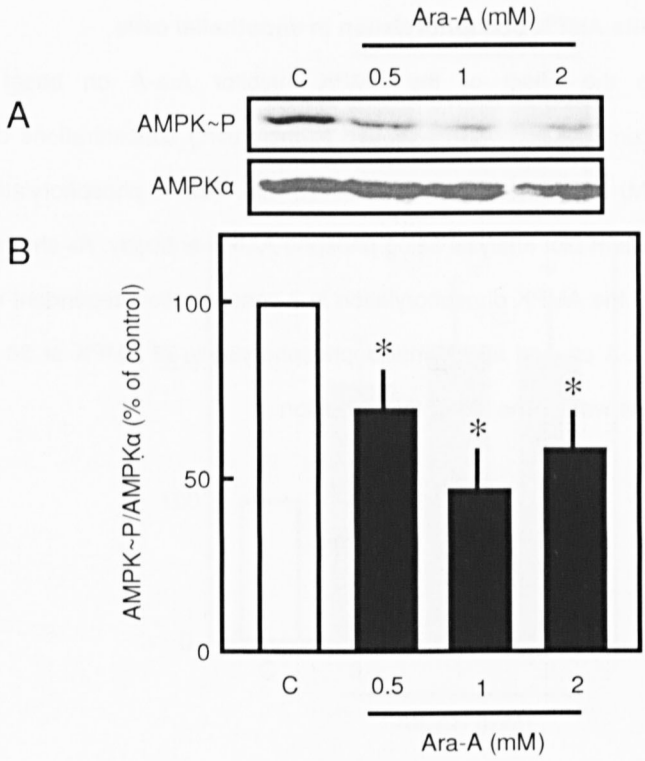


**Fig. 4.8** Effect of Ara-A on AMPK phosphorylation at Thr172 in endothelial cells under basal conditions. Cultured endothelial monolayers were exposed to Ara-A for 30 min at room temperature. **A)** Representative Western blots with an anti-phospho-Thr172 AMPK or anti-total AMPKα antibody. **B)** Densitometric analysis of Western blots. AMPK phosphorylation relative to total AMPKα is given as % increase compared to control (C). The ratio of control was set to 100%. Data are means ± SD of 3-4 separate experiments of independent cell preparations. * $P < 0.05$ vs. C.

### 4.9 AICAR increases AMPK phosphorylation during reperfusion in endothelial cells

As shown in Fig. 4.7, AICAR increased AMPK phosphorylation at Thr172 in EC under basal conditions. To prove whether AICAR is able to activate AMPK also during reperfusion and thereby conferring protection against endothelial barrier failure, endothelial monolayers were exposed to 1 hr hypoxia followed by 45 min of reperfusion. As expected, AMPK phosphorylation increased during hypoxia and dropped back to the normoxic level during reperfusion (Fig. 4.9). Addition of AICAR at the onset of reperfusion prevented the decrease in AMPK phosphorylation during reperfusion. This effect, however, was abolished when EC where reperfused in co-presence of AICAR plus Ara-A (1 mM).

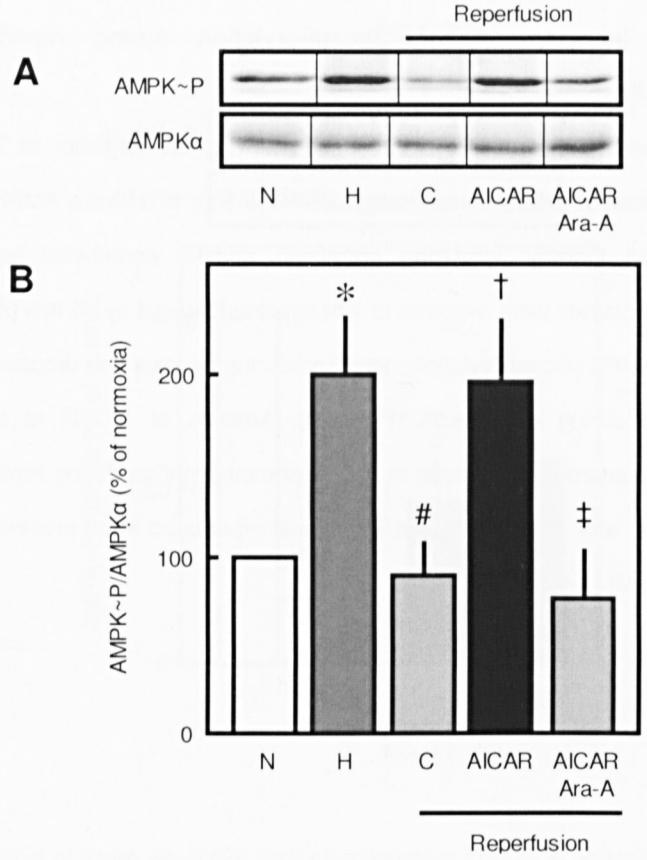


**Fig. 4.9** Effect of AICAR and AICAR plus Ara-A on AMPK phosphorylation during reperfusion in endothelial cells. Confluent endothelial monolayers were exposed to 1 hr hypoxia (H), followed by 45 min reperfusion in the absence (C) or presence of AICAR (1 mM) or AICAR plus Ara-A (1 mM). AICAR plus Ara-A were added at the onset of reperfusion and were present during the whole reperfusion period. **A)** Representative Western blot showing AMPK phosphorylation during normoxia (N), hypoxia (H), or during reperfusion in the absence (C) and presence of AICAR plus

Ara-A. **B)** Densitometric analysis of Western blot. AMPK phosphorylation relative to AMPKα is given as % increase compared to normoxia. The ratio of normoxia was set to 100%. Data are means ± SD of 3-4 separate experiments of independent cell preparations. *P < 0.05 vs. N; #P < 0.05 vs. H; † P < 0.05 vs. C; ‡ P < 0.05 vs. reperfusion plus AICAR.

### 4.10 Activation of AMPK reduces gap formation between adjacent endothelial cells during reperfusion

Here it was hypothesized that pharmacological activation of AMPK by AICAR might have the potential to protect against reperfusion-induced barrier failure. To test this, endothelial monolayers were exposed to 40 min hypoxia ($Po_2$ < 1 mmHg) followed by 30 min of reperfusion ($Po_2$ = 140 mmHg) and intercellular gap formation were analyzed as described in the methods section. Hypoxia (H) caused an immediate increase in intercellular gap formation that was further enhanced by reperfusion. To analyze whether targeted activation of AMPK can reduce reperfusion-induced intercellular gap formation, reperfusion medium was supplemented with 1 mM AICAR. As depicted in Fig. 4.10, AICAR significantly decreased reperfusion-induced intercellular gap formation in endothelial cell monolayers when compared to untreated cells. The role of AMPK activation in AICAR-mediated endothelial barrier stabilization was proven using AMPKα1/2 siRNA. To analyze this, endothelial monolayers were transfected with AMPKα1/2 specific siRNA or negative control siRNA 48 hrs prior to the application of HR. siRNA mediated downregulation of AMPKα1/2 protein not only further enhanced the reperfusion-induced intercellular gaps but also abolished the

beneficial effect of AICAR in reducing reperfusion-induced gap formation, confirming the protective role of AMPK during HR.

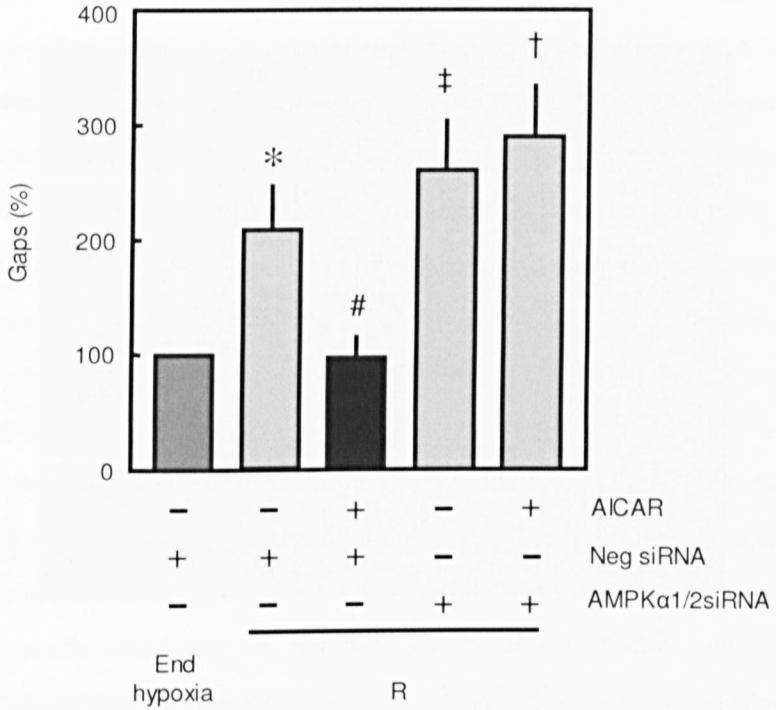


**Fig. 4.10** Effect of AICAR on reperfusion-induced increase of interendothelial gap formation. In a set of experiments cultured endothelial cells were transfected with 25 nM AMPKα1/2 siRNA or negative control siRNA (Neg siRNA). Endothelial monolayers were exposed to 40 min hypoxia followed by 30 min reperfusion (R) in the absence (-AICAR) or presence of AICAR. AICAR was applied at the onset of reperfusion and was present during the whole period of reperfusion. End-hypoxic value was set to 100%. Data are means ± SD of 3-4 separate experiments with independent cell preparations. *$P<0.05$ vs. End hypoxia, #R plus AICAR vs. R alone, ‡R plus AMPKα1/2 siRNA vs. End hypoxia, †R plus AICAR plus AMPKα1/2 siRNA vs. R plus AICAR.

### 4.11 *Activation of AMPK prevents loss of adherens junction proteins from the cell borders and inhibits AMPK translocation into nucleus during reperfusion*

HR is known to alter the location of junction proteins i.e VE cadherin/β-catenin and displayed reduced cell-cell contacts in endothelial cell monolayers (Khaidakov et al., 2010). Here it was analyzed whether activation of AMPK by AICAR prevents reperfusion-induced loss of VE-cadherin/β-catenin from the cell borders. Fig. 4.11 shows that VE-cadherin and β-catenin is continuously localized at the cell borders under normoxic conditions. However, both become discontinuous during hypoxia and reperfusion, indicating adhesion junction disassembly. Treatment of endothelial monolayers with AICAR at the onset of reperfusion prevents the loss of VE-cadherin/β-catenin from the cell borders, indicating that adherens junctions are maintained. Most importantly, AICAR (1 mM) clearly abolished the detrimental effects induced by reperfusion. As shown in Fig. 4.11, Ara-A, a pan-specific pharmacological AMPK inhibitor, abolished the stabilizing effect of AICAR on cell junctions during reperfusion.

Localization of AMPK was also analyzed by immunofluorescence confocal microscopy in endothelial cell monolayers. Under normoxia, AMPK α1 was mainly detected in the cytoplasm of cells. AMPK α2 was found in the cytoplasm as well as in the nucleus. During reperfusion, both isoforms were translocated into the nucleus, even though the effect on AMPKα2 was remarkably higher. Addition of AICAR at the onset of reperfusion prevented the reperfusion-induced translocation of AMPK into the nucleus, which was abolished by Ara-A. Since the nucleus generally occupies a small fraction of the cell volume, small changes in the nuclear: cytoplasm ratio may reflect a gross increase of the nuclear AMPK content.

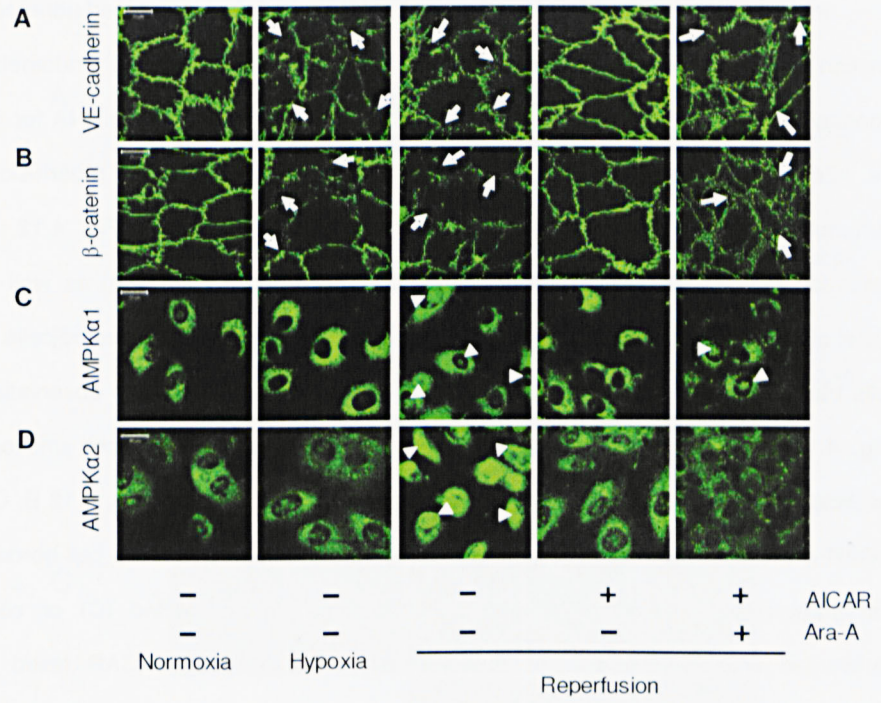


**Fig. 4.11** Effect of AICAR or AICAR plus Ara-A on VE-cadherin, β-catenin and the AMPK α1 or AMPK α2 localization in endothelial cells during reperfusion. Images of confocal microscopy of fluorescently labeled VE-cadherin **(A)**, β-catenin **(B)**, AMPKα1 **(C)** and AMPKα2 **(D).** Endothelial monolayers were exposed to 1 hr hypoxia ($Po_2$ < 5 mm Hg) followed by 45 min reperfusion. Normoxic control cells ($Po_2$ = 140 mm Hg) were left untreated (Normoxia). AICAR (1mM) or AICAR plus Ara-A (1 mM) was added at the onset of reperfusion. Arrows denote loss of VE-cadherin and β-catenin at cell borders. Arrowheads denote translocation of AMPKα1 and AMPKα2 into nucleus. One representative image of 3 independent experiments is shown. Bar = 20 μm.

In the next step the protective effect of AICAR on reperfusion-induced adherens junction disassembly was analyzed in AMPKα1/2 siRNA transfected endothelial monolayers. Cells were transfected with AMPKα1/2 siRNA or negative siRNA for 48 hrs. Afterwards they were exposed to 1 hr of hypoxia followed by 45 min reperfusion. Immunofluorescence staining with antibodies specific for AMPKα1 (Fig. 4.12 A) confirmed the downregulation of AMPKα protein contents in cytoplasm as well in nuclei of AMPKα1/2 siRNA transfected cells as compared with non-transfected cells or cells transfected with negative control siRNA. Consistent with the above observation (Fig. 4.11 A, B), VE-cadherin and β-catenin vanished from the cell-cell junctions resulting in the formation of interendothelial gaps during reperfusion (Fig. 4.12 B, C). AICAR prevented the loss of both, VE-cadherin and β-catenin, from the cell borders and showed stabilization of adherens junctions in non-transfected (C) or cells transfected with negative siRNA during reperfusion. However, AICAR failed to stabilize the adherens junctions in AMPKα1/2 siRNA transfected cells, indicating that the action of AICAR was mainly transduced by AMPK.

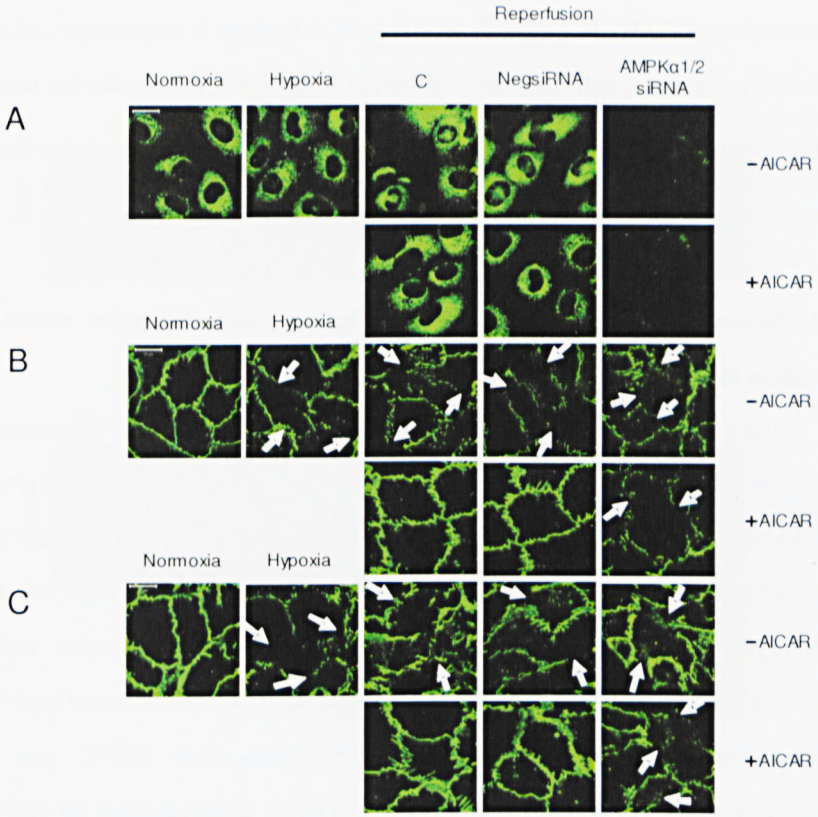


**Fig. 4.12** Effect of AICAR on AMPK α1, VE-cadherin, and β-catenin localization in AMPK α1/2 siRNA transfected endothelial cells during reperfusion. Images of confocal microscopy of fluorescently labeled **(A)** AMPKα1, VE-cadherin **(B)**, and β-catenin **(C)**. Endothelial cell monolayers were exposed to 1 hr hypoxia ($Po_2$ < 5 mm Hg) followed by 45 min reperfusion. Normoxic control cells ($Po_2$ = 140 mm Hg) were left untreated (Normoxia). In a set of experiments cells were left non-transfected or were transfected with 25 nM siRNA targeted against AMPKα1/2 or negative control siRNA (Neg siRNA). The AMPK activator AICAR (1 mM) was given at the onset of reperfusion. Cells were

left untreated (-AICAR), treated with AICAR (+AICAR) alone in non-transfected cells (C) or in cells transfected with AMPKα1/2 siRNA or Neg siRNA. Arrows denote loss of VE-cadherin and β-catenin at cell borders. One representative image of 3 independent experiments is shown. Bar = 20 μm.

### 4.12 Activation of AMPK reduces reperfusion-induced F-actin stress fiber formation in endothelial cells

The increase in HR-induced endothelial permeability has been associated with F-actin reorganization in endothelial monolayers (Lum et al., 1992); this parameter of cyto-architecture was also analyzed here. Endothelial monolayers exposed to 1 hr hypoxia followed by 45 min reperfusion showed apparent changes in actin localization. Under normoxic conditions, EC showed a cortical F-actin localization while HR increased formation of long, cell-traversing stress fibers. AICAR reduced reperfusion-induced F-actin stress fiber formation, but failed when AMPK was either pharmacologically inhibited by Ara-A (Fig. 4.13 A) or downregulated by AMPKα1/2 siRNA (Fig. 4.13 B).

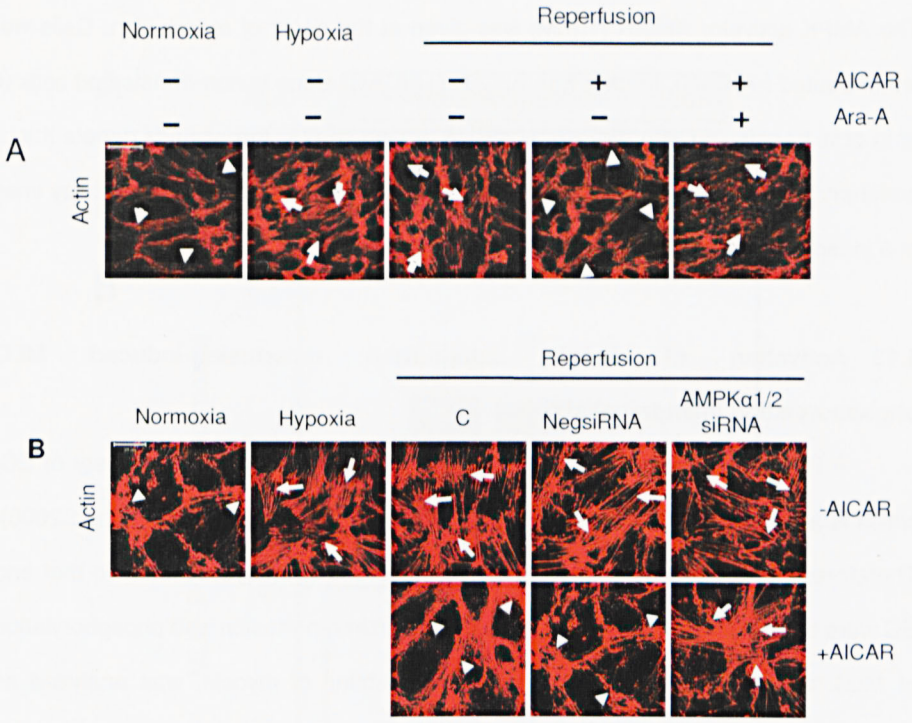


**Fig. 4.13** Effect of AICAR on F-actin localization in presence and absence of Ara-A or in AMPK α1/2 siRNA transfected endothelial cells during reperfusion. Endothelial cell monolayers were exposed to 1 hr hypoxia ($Po_2$ < 5 mm Hg) followed by 45 min reperfusion. Normoxic control cells ($Po_2$ = 140 mm Hg) were left untreated (Normoxia). **(A)** The AMPK activator AICAR (1 mM) was added alone or in combination with Ara-A (1 mM) at the onset of reperfusion. Controls were left untreated (-AICAR). One representative confocal microscopy image of 3 independent experiments is shown. Bar = 50 μm. **(B)** In a set of experiments cells were left non-transfected or were transfected with 25 nM siRNA targeted against AMPKα1/2 or negative control siRNA (Neg siRNA).

The AMPK activator AICAR (1 mM) was given at the onset of reperfusion. Cells were left untreated (-AICAR), treated with AICAR (+AICAR) alone in non-transfected cells (C) or in cells transfected with AMPKα1/2 siRNA or Neg siRNA. Arrowheads denote the cell periphery and arrow F-actin stress fiber. One representative confocal microscopy image of 3 independent experiments is shown. Bar = 20μm.

### 4.13 Activation of AMPK antagonizes reperfusion-induced MLC phosphorylation in endothelial cells

It has been shown that reperfusion activates the contractile machinery of EC, which is an important determinant of endothelial gap formation (Gündüz et al., 2006). Therefore, the role of AMPK in this activation process is analyzed here. To that end EC were exposed to 1 hr hypoxia followed by 45 min reperfusion and phosphorylation of MLC, the low molecular weight regulatory subunit of myosin, was analyzed as indicator of the activation state of the contractile machinery. Western blot analysis shows (Fig. 4.14) that HR led to an increase in MLC phosphorylation. However, addition of AICAR at the onset of reperfusion abolished the reperfusion effect on MLC phosphorylation. To test whether the effect of AICAR on reperfusion-induced MLC phosphorylation is mediated by AMPK, AICAR was added in combination with Ara-A at the onset of reperfusion. As shown in Fig. 4.14, Ara-A abolished the effect of AICAR on reperfusion-induced MLC phosphorylation, indicating that that activation of AMPK is capable to antagonize reperfusion-induced activation of the contractile machinery in EC.

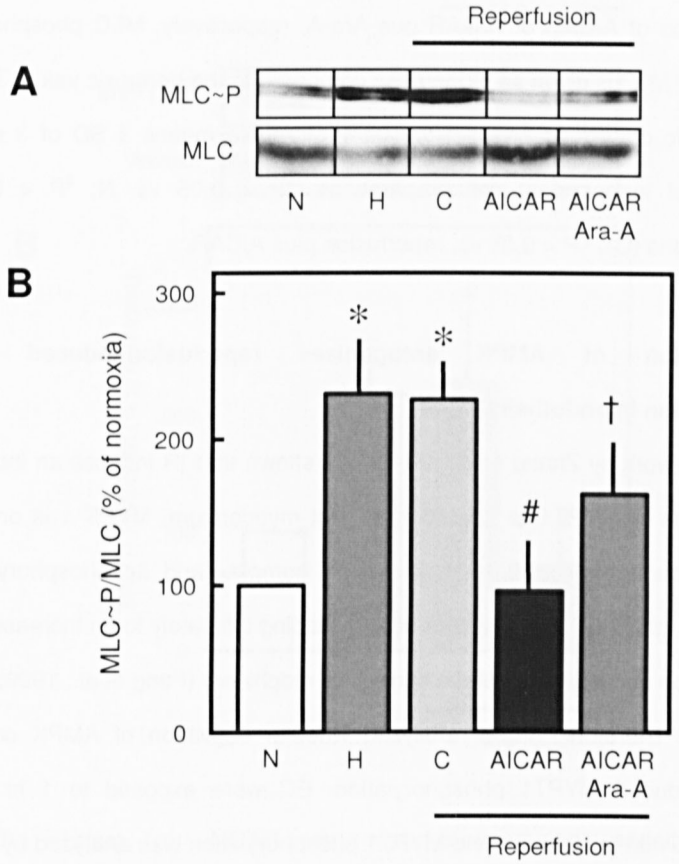


**Fig. 4.14** Effect of AICAR on reperfusion-induced endothelial Myosin light chain (MLC) phosphorylation. Confluent endothelial monolayers were exposed to 1 hr hypoxia (H) followed by 45 min reperfusion in the absence or presence of AICAR (1 mM) or AICAR plus Ara-A (1mM). AICAR and Ara-A were added at the onset of reperfusion and was present during the whole reperfusion period. **(A)** Representative Western blots using an anti-phospho-Ser19 MLC antibody. **(B)** Densitometric analysis of MLC phosphorylation under normoxia (N), hypoxia (H), reperfusion in the absence

(C) or presence of AICAR or AICAR pus Ara-A, respectively. MLC phosphorylation relative to total MLC is given as % increase compared to the normoxic value. The ratio under normoxic conditions was set to 100%. Data are means ± SD of 3 separate experiments of independent cell preparations. *P < 0.05 vs. N; #P < 0.05 vs. reperfusion alone (C); † P < 0.05 vs. reperfusion plus AICAR.

### 4.14 Activation of AMPK antagonizes reperfusion-induced MYPT1 phosphorylation in endothelial cells

Recent work by Zhang et al. (2010) has shown that IR induces an increase in phosphorylation of MYPT1 at Thr850 in the rat myocardium. MYPT 1 is one of the regulatory subunit of the MLPC holoenzyme complex and its phosphorylation is established to inhibit the phosphatase activity leading ultimately to an increase in MLC phosphorylation and activation of the contractile machinery (Feng et al., 1999; Velasco et al., 2002). Therefore, it was analyzed whether activation of AMPK can affect reperfusion-induced MYPT1 phosphorylation. EC were exposed to 1 hr hypoxia followed by 45 min reperfusion and MYPT1 phosphorylation was analyzed by Western blot. AICAR was added at the onset of reperfusion and remained throughout the reperfusion period. Fig 4.15 shows that HR provoked a significant increase of MYPT1 phosphorylation at Thr850. However AICAR reduced the reperfusion-induced phosphorylation of MYPT1 at Thr850 below the normoxic level.

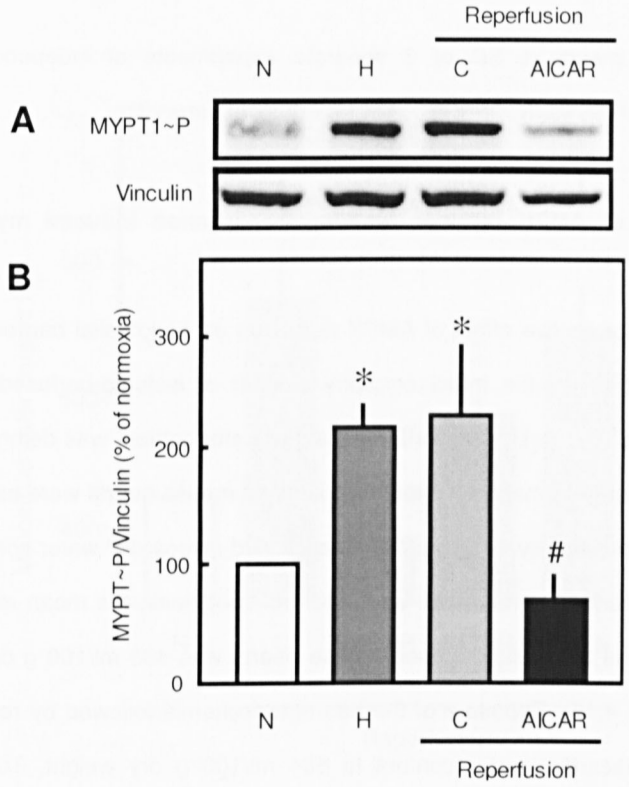


**Fig. 4.15** Effect of AICAR on reperfusion-induced endothelial MYPT1 phosphorylation. Confluent endothelial monolayers were exposed to 1 hr hypoxia followed by 45 min reperfusion in the absence or presence of AICAR (1 mM). AICAR was added at the onset of reperfusion and was present during the whole reperfusion period. **(A)** Representative Western blot showing MYPT1 phosphorylation using an anti-phospho-Thr850 MYPT1 antibody. **B)** Densitometric analysis of MYPT1 phosphorylation under normoxia (N), hypoxia (H), reperfusion in the absence (C) or presence of AICAR, respectively. MYPT 1 phosphorylation relative to vinculin is given as % increase compared to normoxic value. The ratio under normoxia was set to

100%. Data are means ± SD of 3 separate experiments of independent cell preparations. *P < 0.05 vs. N; # P < 0.05 vs. reperfusion alone (C).

### 4.15 Activation of AMPK reduces ischemia-reperfusion induced myocardial water content

Finally, the protective effect of AMPK activation on endothelial barrier function under IR was proven in the intact coronary system of isolated-perfused isolated mouse hearts according to Langendorff. Myocardial water content was determined as index for tissue edema formation. To test this, isolated mouse hearts were exposed to 60 min ischemia followed by 40 min of reperfusion and myocardial water content was determined as described in methods. Under control conditions, the mean myocardial water content of the normoxic perfused mouse hearts was 433 ml/100 g dry weight after 100 min (Fig 4.16). Exposure of the hearts to ischemia followed by reperfusion increased the myocardial water content to 584 ml/100 g dry weight. To analyze whether pharmacological activation of AMPK can reduce IR-induced increase in myocardial water content, reperfusion medium was supplemented with 0.5 mM AICAR, a concentration only half that applied in the cell culture model. AICAR markedly reduced the reperfusion-induced increase in myocardial water content. This effect of AICAR was abrogated, if the hearts were reperfused in the co-presence of AICAR plus Ara-A. Ara-A alone did not affect myocardial water content compared to the reperfusion group.

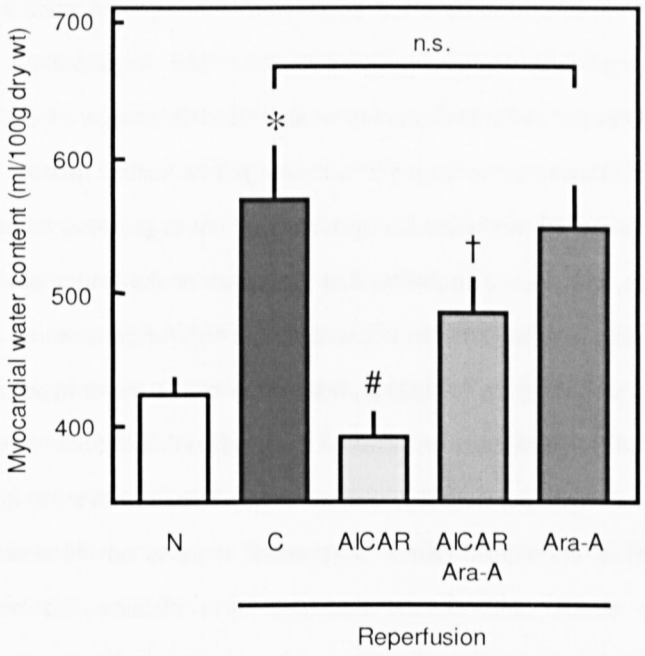


**Fig. 4.16** Effect of AICAR on myocardial water content of the isolated saline-perfused mouse hearts after ischemia-reperfusion. Hearts were exposed to 60 min of no-flow ischemia followed by 40 min of reperfusion (C) or 100 min of normoxia (N). AICAR (0.5 mM) was added into the medium at the onset of reperfusion in the absence or presence of Ara-A (1 mM). Data are means ± SD of 4-5 separate experiments with independent organ preparations. $^{*}P < 0.05$ vs. N; $^{\#}P < 0.05$ vs. reperfusion alone (C); $^{\dagger}P < 0.05$ vs. reperfusion plus AICAR; n.s., not significantly different.

## 5. Discussion

Numerous vascular disorders are associated with impaired endothelial barrier function promoting inflammation, atherosclerosis, and myocardial dysfunction (Rodrigues and Granger 2010; Dongaonkar et al., 2010; Celermajer et al., 1992). HR has also been demonstrated to cause endothelial barrier failure leading to capillary leakage, edema formation, and vascular dysfunction (Lum et al., 1992; Lum and Malik, 1996). At present, it is well established that activation of the endothelial contractile machinery and disruption of adherens junctions are key steps towards opening of intercellular gaps and, thus, barrier failure under many conditions of hyperpermeability. Until now many efforts have been undertaken to elucidate those processes involved in the development of hyperpermeability. Comparatively little, however, is known about maneuver to protect endothelial barrier. At present, there is no therapeutic strategy available, which directly acts on the endothelium to stabilize the barrier under physiological conditions and/or to protect it against permeability stress under pathophysiological conditions.

In the present study, the role of AMPK on endothelial barrier function was studied. The data demonstrate that AMPK is a novel protective signaling element, which is involved in the control of endothelial barrier function under physiological condition and can protect against an imminent failure under permeability stress. Reduction of the endothelial AMPK protein expression led to disruption of cell adhesion junctions, increase in F-actin stress fiber formation and an increase in basal endothelial permeability. On the other hand, targeted activation of AMPK led to inactivation of the endothelial contractile machinery, rearrangement of F-actin cytoskeleton, attenuation of

adherens junction disassembly, and prevented reperfusion-induced barrier failure. In detail, the major findings of the present study are:

(1) Downregulation of AMPK protein content by gene silencing increased basal permeability of endothelial monolayers, disturbed adherens junctions and increased actin stress fiber formation. Comparable effects were elicited in response to combined downregulation of the α1 plus α2 isoform of AMPK or when either, the α1 or α2 isoform was downregulated, separately.

(2) Hypoxia increased AMPK phosphorylation in endothelial cells. During reperfusion, however, phosphorylation declined towards basal level within min. Pharmacological activation of AMPK by AICAR at the onset of reperfusion prevented the decline in AMPK phosphorylation and reduced reperfusion-induced intercellular gap formation in endothelial monolayers. This protective effect on barrier function was abolished if both isoforms of AMPK α subunit had been reduced by siRNA.

(3) Hypoxia caused disturbance of cell adhesion structures, as determined by loss of VE-cadherin and β-catenin at sites of cell-cell contacts of endothelial monolayers. This effect was further enhanced during reperfusion. Activation of AMPK by AICAR, added at the onset of reperfusion, inhibited the reperfusion-evoked morphological changes of adherens junctions. This protective effect of AICAR failed when Ara-A, a pharmacological inhibitor of AMPK, was added together with AICAR. AICAR also failed to protect, when both isoforms of AMPKα subunit had been reduced in endothelial cells by siRNA.

(4) Activation of AMPK by AICAR blocks reperfusion-induced actin stress fiber formation in endothelial cells.

(5) During reperfusion AMPKα1 and AMPKα2 were translocated from cytoplasm to the nucleus. This reperfusion-induced translocation of both AMPKα isoforms was prevented by AICAR.

(6) Hypoxia increased phosphorylation of MLC and MYPT1, the phosphorylation state of which persisted even during reperfusion. AICAR reduced the reperfusion-induced phosphorylation of MLC and MYPT1.

(7) Ischemia-reperfusion increased myocardial water in a model of isolated-perfused mouse heart. AICAR reduced the reperfusion-induced accumulation of myocardial water.

### 5.1 Reduction of AMPK α1/2 protein and its isoforms induces endothelial barrier failure

Recently, it has been shown that expression of a dominant negative AMPK increased permeability of cultured endothelial monolayers (Dixit et al., 2008). Furthermore, these monolayers responded with a significant higher increase in permeability when challenged with tumor necrosis factor α, indicating that the reduction of AMPK activity affect basal barrier function and enhances its vulnerability to permeability stress. These findings are in accordance with work from several other research groups, which show that AMPK is involved in the regulation of the architecture of epithelial cells (Lee et al., 2007; Mirouse et al., 2007). Therefore, in the present study the hypothesis was tested whether inhibition of AMPK activity affects endothelial adhesion structures and enhances macromolecule permeability of endothelial monolayers. Downregulation of AMPK protein content by AMPKα1/2 specific siRNA demonstrated a functional role of the kinase in endothelial barrier failure. Reduction of both AMPKα isoforms was

accompanied by an increase in basal macromolecule permeability compared to control-transfected monolayers. Furthermore, reduction of AMPKα1/2 protein also led to the disintegration of VE-cadherin/β-catenin-mediated cell adhesion structures and formation of actin stress fibers in the endothelial monolayers.

It is well documented that endothelial permeability is regulated in part by dynamic opening and closure of adherens junctions, which are composed of VE-cadherin, anchored to numerous cytoplasmic molecules including β-catenin via its cytoplasmic tail. It has been shown that dissociation of VE-cadherin and β-catenin results in the increased macromolecule permeability of the endothelial monolayers (Navarro et al., 1996). Therefore, the fact that loss of AMPKα1/2 protein results in disorganization of endothelial adhesion structures and increases macromolecule permeability indicates that this kinase is a key element in the regulation of barrier property.

To evaluate which AMPK isoform is responsible for the regulation of permeability, EC were transfected with siRNA specifically targeting either AMPKα1 or AMPKα2 isoform. Interestingly, downregulation of AMPK α1 or AMPK α2 protein alone, significantly increased monolayer permeability compared to cells transfected with negative control siRNA. This strongly suggests that endothelial barrier is critically regulated by both isoforms of AMPK α. Moreover, downregulation of only one AMPK α isoform led to loss of VE-cadherin and β-catenin at cell borders and increase of actin stress fiber formation, similar to alterations observed in AMPKα1/2 depleted EC. The coincidental silencing of both isoforms of AMPK α resulted in an approximately 3-4-fold increase in endothelial permeability, whereas silencing of either isoform, AMPKα1 or AMPKα2 alone, caused only 2-fold increases in endothelial permeability. The

comparison of these two different regimes of AMPK downregulation suggests that both isoforms contribute to the regulation of endothelial barrier function, and each isoform is able to partially compensate for lack of function of the other isoform. It is unclear whether their contribution is transferred by the same mechanism. Nevertheless, these findings strongly emphasize the important role of AMPK in the regulation of endothelial barrier function.

## 5.2 Activation of AMPK reduces reperfusion-induced interendothelial cell gap formation

In spite of the clear benefit, reperfusion itself can cause a serious injury in heart, as well as in other organs, through a cascade of adverse mechanisms (Bonventre, 1993; Garcia-Dorado and Piper, 2006). This specific reperfusion injury adds on the deleterious processes elicited during the preceding ischemic period. Because of its unpredictable occurrence, ischemia usually defies any therapeutic intervention (Piper et al., 2004). In contrast, reperfusion, most commonly induced during clinical intervention, provides an opportunity to prevent further injury. This concept of IR injury, originally adopted on the whole organ injury, has been translated to endothelial barrier function. Several *in vitro* and *in vivo* studies have demonstrated that barrier function is also impaired during HR, leading to an increased in endothelial permeability (Inauen et al., 1990; Witt et al., 2003). The detailed analysis has shown that ischemia disturbes endothelial barrier by opening of gaps between adjacent EC, and this process is further accelerated by reperfusion (Gündüz et al., 2006; Kasseckert et al., 2009).

In the present study it was tested whether the targeted activation of AMPK can prevent the deleterious effect on barrier function induced by reperfusion. The data show

that activation of AMPK by AICAR at the onset of reperfusion abrogates reperfusion-induced increase of intercellular gap formation, while downregulation of AMPKα protein content not only abolished this beneficial effect of AICAR, but also further enhanced the reperfusion-induced gap formation. The ability of AICAR to abrogate reperfusion-induced increase in permeability can be of special therapeutic interest, because targeted AMPK activation may be applied if barrier failure is imminent during pathophysiological conditions.

The concept of organ protection by targeted activation of AMPK is supported by many reports. Studies performed in mice, rat and dogs have confirmed the protective effect of AMPK activation on myocardial injury (Calvert et al., 2008; Bhamra et al., 2008; Sasaki et al., 2009). Pavia et al. (2010) show that transitory activation of AMPK at the first minutes of reperfusion protects the ischemic-reperfused rat myocardium against infarction, suggesting that AMPK activation could be critical in determining the outcome of reperfusion injury. Recently, Kim et al. (2011) have also shown that direct AMPK activation preserves the energy change during ischemia and protects mouse hearts against IR injury by reducing myocardial apoptosis and necrosis. Thus, the protective effect has been related to the AMPK-mediated maintenance of energy metabolism and prevention of necrosis as well as apoptosis of cardiomyocytes. The results of the present study demonstrate the importance of AMPK activation for the maintenance of endothelial barrier function. If the data obtained in the model of cultured endothelial cells are extrapolated to the vascular system of the whole heart, one can speculate that activation of AMPK at the onset of reperfusion may prevent a further increase in capillary leakage and myocardial edema which can jeopardize the outcome of reperfusion.

### 5.3 Activation of AMPK reduces the loss of VE-cadherin and β-catenin at the cell–cell borders during reperfusion in endothelial cells

Previous studies have shown that HR induces endothelial barrier failure by disrupting the integrity of adherens junctions, leading to increased endothelial permeability (Lampugnani and Dejana, 1997; Khaidakov et al., 2010). The present study provides compelling evidence that AMPK is involved in regulation of cell adhesion, because it is clearly demonstrated that AICAR prevents the loss of adherens junction proteins, i.e VE-cadherin/β-catenin, at cell borders and maintains endothelial integrity during reperfusion. In the current study it was analyzed whether AMPK signaling can affect reperfusion-evoked disturbance of adherens junction morphology. Immunocytochemical staining shows that VE-cadherin and β-catenin were nicely decorated at cell borders in normoxic EC that became discontinuous during HR, indicating the disassembly of the adhesion junctions. However, endothelial monolayers treated with AICAR clearly abolished the detrimental effect induced by HR and enhances the endothelial barrier function by facilitating the assembly of adhesion junctions. The protective effect of AICAR was completely abolished in AMPK depleted EC, which suggest that specific AMPK activation is necessary for this protective effect.

The findings of the present study are supported by previous work from Zhang et al., (2006) and Zheng & Cantley (2007) showing that the activation of AMPK by AICAR facilitates the assembly of tight junctions, increased transendothelial resistance and decreased permeability in monolayers of an epithelial cell line from dog kidney (MDCK cells) under basal culture conditions. The present study differs from previous work in a way that we used a well-established endothelial cell monolayer model to demonstrate the effect of AICAR on the assembly of adherens junction proteins even under

conditions of HR stress. The underlying mechanism, however, is still not fully understood. The analysis of the precise molecular mechanism, how AICAR can *preserve the association of the VE-cadherin/β-catenin complex under HR conditions*, is beyond the scope of the present study.

A possible explanation for the protective effect of AMPK activation on cell adhesion, and beyond, may come from studies which show that β-catenin protein is *necessary* not only for the stable cell-cell adhesion but also plays a crucial role in the Wnt signaling pathway, which is involved in angiogenesis, cell growth and anti-apoptotic pathways (Willert and Nusse, 1998). Zhao et al. (2010) has recently found that AMPK induces the phosphorylation of β-catenin at Ser552, which enhances its transcriptional activity and retards its degradation (Daugherty and Gottardi, 2007). This stabilization could be one of the possible mechanisms that might be involved in AICAR-induced preservation of cell adhesion structures even under HR conditions. Taken together these results raise the interesting possibility that targeted activation of AMPK during conditions of energy stress stabilizes contacts between the cells.

## 5.4 AICAR prevents nuclear translocation of AMPK during reperfusion in endothelial cells

Based on a previous observation that intracellular localization of AMPK is regulated by different factors, including oxidative stress (Kodiha et al., 1997), interest was focused on the distribution of AMPK during HR. Immunocytochemical analyses in this study show for the first time that α1 isoform of AMPK remains mainly in the cytoplasm while α2 was found in the cytoplasm as well as in the nuclei of normoxic and hypoxic EC. When cells were exposed to reperfusion, the levels of both isoforms were

increased in the nuclei. However, AMPKα2 translocation was much more pronounced. Addition of AICAR at the onset of reperfusion prevented the reperfusion-induced translocation of both AMPKα isoforms. The molecular mechanism underlying the reperfusion-induced nuclear translocation of AMPKα was not further analyzed in the present study. However, it appears that the reperfusion-induced dephosphorylation of the AMPK is involved in nuclear translocation of this enzyme. This assumption is supported by the following observations. Firstly, hypoxia increases AMPK phosphorylation at Thr172 and the protein is retained in the cytoplasm. During reperfusion AMPK is dephosphorylated and this coincides with AMPK translocation into the nucleus. Secondly, pharmacological activation of AMPK by AICAR at the onset of reperfusion prevents AMPK dephosphorylation at Thr172 and, again, AMPK did not enter the nucleus. In line with this observations, it has been previously demonstrated that dephosphorylation of the $\beta_1$ subunit of AMPK is associated with the nuclear redistribution in HEK-293 cells (Warden et al., 2001). However, it is not yet clear for AMPK complexes containing the other subunits.

AMPK regulates the expression of a large number of genes involved in different cellular processes that are essential for the cell survival (Lee et al., 2007; Yang et al., 2001). Moreover, AMPK is also known to interact with various transcription factors namely p300/CBP, members of the FOXO family, p53 and NFκ-B (Towler and Hardie, 2007; Yang et al., 2001), hence, proper sub-cellular localization of AMPK is required to interact and regulate these proteins. The mechanism of AMPK activation is fairly clear, but little is known about nuclear and cytoplasmic pools and the regulatory mechanism governing the intracellular localization of AMPK during HR and other pathophysiologcal conditions. This type of regulated AMPK distribution should be critical for the proper

response to various cellular stimuli, leading to phosphorylation of its multiple downstream targets in the cells. It is very important to gain insights to understand this mechanism because such knowledge will open the door to identify specific AMPK functions in different cellular compartments, including maintenance of cytoskeleton and cell adhesion structures, during physiological and pathophysiological changes.

### 5.5 Activation of AMPK antagonizes reperfusion-induced MLC and MYPT1 phosphorylation in endothelial cells

MLC is a regulatory component of the endothelial contractile machinery and its phosphorylation has been suggested a measure of endothelial force development by Sheldon and co-workers (1993), increased gap formation and endothelial permeability (Garcia et al., 1995). Since IR is also known to activate the contractile machinary of EC through MLC phosphorylation and causes intercellular gap formation (Gündüz et al., 2006), this parameter of contractile activation was also analyzed in the present study. It is clearly demonstrated here that AICAR significantly abolished reperfusion-induced MLC phosphorylation in EC. This decrease in MLC phosphorylation is accompanied by a reduction in reperfusion-induced intercellular gap formation (Fig. 4.10), which explains mechanistic aspects of the endothelial barrier stabilization. AICAR treatment at the onset of reperfusion abolished the MLC phosphorylation through AMPK because the effect of AICAR on reperfusion-induced MLC phosphorylation was significantly reduced in EC treated with AMPK inhibitor Ara-A. In line with our current findings, a recent study has also shown that activation of AMPK by AICAR attenuates smooth muscle cells contraction by dephosphorylating MLC through a Rho/ROCK pathway (Wang et al., 2011).

Presently the exact mechanism underlying the effect of AICAR on reperfusion-induced contractile machinery in EC is not well understood and needs to be elucidated by further studies. It has previously been shown that activation of phosphoglycerate kinase signaling (PKG) pathway results in dephosphorylation of MLC in isolated vessels via MLCP activation (Nakamura, 2007). As discussed above, AMPK interacts with a variety of cellular targets so the signaling pathways responsible for the protective effects of AICAR administration seems to be very complex. However, several studies have demonstrated that activation of AMPK resulted in increased eNOS phosphorylation that enhanced eNOS activity and NO bioavailability in EC (Morrow et al., 2003; Zhang et al., 2006). Moreover, activation of cGMP/PKG signaling is also shown to decrease the oxidative stress, ionomycin or thrombin induced endothelial barrier failure (Hempel et al., 1998; Draijer et al., 1995). A recent study by Kasseckert et al. (2009) clearly showed that stimulation of the cGMP/PKG signaling at the onset of reperfusion markedly reduces the intercellular gap formation by attenuating cytosolic calcium overload and inactivation of endothelial contractile machinery, which ultimately protects against myocardial edema. Therefore one can assume that activation of AMPK by AICAR, in part, may reduce reperfusion-induced MLC phosphorylation via cGMP/PKG mediated pathway but the specific mechanism remains to be elucidated.

As discussed earlier, activation of the endothelial contractile machinery is primarily controlled by the phosphorylation of MLC that is regulated by balanced activities of MLCP and MLCK. A variety of signaling mechanisms have been suggested to be involved in the regulation of MLCP activity including phosphorylation of MYPT1 at two threonine residues i.e Thr696 and Thr850 (Feng et al., 1999; Birukova et al., 2004; Härtel et al., 2007). It is also shown that IR induces the

phosphorylation of MYPT1 via Rho kinase (ROCK) and plays an important role in the pathogenesis of heart injury (Zhang et al., 2010). Wang et al. (2011) have recently reported that AMPK activation by AICAR lowers blood pressure by suppressing contractility of smooth muscle cells through inhibiting phosphorylation of MYPT1 and MLC via RhoA inactivation. The results of present study also demonstrate that targeted activation of AMPK by AICAR antagonizes the reperfusion-induced MYPT1 phosphorylation in EC, however the underline mechanism remained uninvestigated. Hartshorne et al. (1998) have proposed that cellular localization of MYPT1 alters upon its phosphorylation by upstream kinases like PKA, which is a major determinant of substrate-specific phosphatase activity. Hence, based on these findings it could be assumed that AMPK may also be involved in the alteration of MYPT1 localization or its confirmation in EC. Thus changes in MYPT1 localization or protein conformation induced by AMPK-mediated phosphorylation may prevent MYPT1 phosphorylation by ROCK, which is critical for MYPT1 activation. Our results indicate that AMPK activation by AICAR antagonizes the effect of reperfusion on MYPT1 phosphorylation.

### 5.6 Activation of AMPK blocks actin stress fiber formation during reperfusion in endothelial cells

Several studies have shown that the increase in endothelial permeability after HR was accompanied by reorganization of the F-actin cytoskeleton (Torri et al., 2007; Lum et al., 1992). Previously, it was found that AMPK could provide a direct link between regulation of metabolic energy and reorganization of the cytoskeleton in an *in vitro* and *in vivo* model. Blume et al. (2007) have demonstrated that AMPK reduces F-actin assembly, defective stress fiber formation, and alters cell morphology by increasing

VASP phosphorylation. The present study clearly showed the cortical localization of actin under normoxic conditions whereas HR provoked F-actin stress fiber formation in EC. The loss of actin from cell periphery and disintegration of adherens junctions may result in endothelial gap formation during HR. Plant et al. (2008) has shown that adiponectin, another AMPK activating agent was found to reduce actin stress fiber formation, preserved the localization of actin cytoskeleton as well as endothelial junction proteins. Therefore, the effect of AICAR on reperfusion-induced actin stress fiber formation was tested. Interestingly, the cytoskeletal changes mentioned above were similar to findings in the present study, showing that AICAR clearly blocks reperfusion-induced F-actin stress fiber formation through AMPK activation, but failed, when AMPK was pharmacologically inhibited or downregulated with siRNA.

Binding of adherens junction to the cortical actin is essential for the integrity of endothelial barrier whereas alteration of these structures results in disintegration of endothelial junctions and hyperpermeability of endothelial monolayers (Lampugnani and Dejana, 1997; Fürst et al., 2008). Although, the detailed mechanism of AICAR-induced preservation of the actin cytoskeleton during reperfusion remains to be elucidated, work from different laboratories may provide a plausible explanation. It is well established that reactive oxygen species (ROS) generated during HR by all cell of the cardiovascular system is an important determinant for the endothelial barrier function, microvascular function and tissue injury (Pearlstein et al., 2002; Li and Shah, 2004). The actin cytoskeleton is highly sensitive to ROS, especially under conditions like HR, which has been shown to cause disruption of cortical actin (Lum et al., 1992). Increasing evidence suggests that activation of AMPK reduces intracellular ROS production in different cells types (Li et al., 2009; Zhang et al., 2008). Based on that, it can be speculated that

treatment of AICAR at the onset of reperfusion reduces ROS generation and, hence, decreases F-actin stress fiber formation. However, further studies are needed to verify the concept that targeted activation of AMPK can reduce reperfusion-induced actin stress fiber formation leading to stabilization of endothelial barrier.

## 5.7 Activation of AMPK reduces ischemia-reperfusion induced myocardial water content

The protective effect of AMPK against reperfusion-induced endothelial barrier failure as demonstrated in an *in vitro* model of culture endothelial monolayers was also verified in the intact coronary system of the isolated, saline-perfused mouse heart. Pharmacological activation of AMPK by AICAR led to a marked reduction of the reperfusion-induced increase in myocardial water content, when applied at the onset of reperfusion. The data show that AICAR plays a beneficial role in the stabilization of vascular permeability barrier in the intact coronary system, indicating that its application during reperfusion confers protection to the heart against reperfusion-induced injury. Due to this specific effect on endothelial cells, activation of AMPK may be a promising therapeutic option.

It is well documented that activation of AMPK reduces myocardial infarction size and protects myocardial cells against IR-induced necrosis and apoptosis (Paiva et al., 2009, 2010; Kim et al., 2011). Previous studies have demonstrated that edema formation in response to ischemia and reperfusion compromises cardiac function and can jeopardize the outcome of reperfusion (Kahles et al., 1982; Rubboli et al., 1994; Dongaonka et al. 2012). This edema formation, however, is usually not implicated as important determinant of reperfusion injury. Maneuver targeting endothelial barrier

function, like AMPK activation, may constitute an important tool to prove the implication of the maintenance of endothelial barrier function during pathophysiological conditions like ischemia and reperfusion.

Although, the effects of AMPK inactivation remained unclear on the heart function, transgenic animal models have been widely used to figure out whether AMPK is a friend or a foe during an IR condition. Russell et al. (2004) have reported that AMPKα2-kinase-dead hearts showed an impaired recovery of left ventricular function that led to an increased myocardial injury, apoptosis, and necrosis following IR. Moreover, frequent mutations in AMPK gene have also been associated with cardiomyopathy, cardiac hypertrophy, ventricular preexcitation and conduction abnormalities (Davies et al., 2006; Sidhu et al., 2005) that confirm the importance of AMPK for proper functioning of the heart. A further support for the importance of AMPK activity comes from the work of Liao (2005), demonstrating the reduced level of AMPK activity in hearts from adeponectin deficient mice resulted in an increased hypertrophy and heart failure following transverse aortic constriction.

## 5.8 Future perspective

Ischemia/hypoxia-reperfusion provoked endothelial barrier failure causes vascular leakage which enhances extravasation of water, solutes, macromolecules and blood cells into interstitial tissue leading to edema formation. It causes flooding of the organ, which can produce tissue damage, organ failure or even death. The present study shows that targeted activation of AMPK reduces reperfusion-induced endothelial barrier failure and protects the heart against reperfusion-induced edema. Although the AMPK is traditionally known as a sensor of energy status that regulates

the cellular metabolism (Hardie, 2007), recent discoveries have now provided novel evidence that this kinase is also involved in the regulation of cellular architecture and vascular permeability (Zheng and Cantley, 2007; Dixit et al., 2008). AMPK activating agents have emerged novel therapeutic strategies for human diseases in recent years (Beauloye et al., 2011). However, there are various hindrances that still need to be overcome to transform our knowledge into clinical practice. Need of the hour is to identify safer drugs that specifically activate AMPK and give therapeutic advantages over the existing one by having diminished side effects. Hence, development of specific pharmacological activators for AMPK might be an important innovation to block vascular leakage during pathophysiological conditions. In the present study we have used an *in vitro* and *ex vivo* model of ischemia and reperfusion, which can only partially reproduce the *in vivo* conditions. Therefore, an appropriate *in vivo* model and well-designed clinical trials would help to validate the pathophysiological relevance of the current finding during ischemia-reperfusion.

In summary, the present study revealed AICAR as a potent endothelial barrier-protecting agent during reperfusion. It is also shown here that adherens junction and the contractile machinery are important subcellular systems targeted by AMPK when activated by AICAR during reperfusion. Most importantly, results of the present study provide experimental evidence for the use of AICAR as an interesting pharmacological strategy to preserve the tissue function by reducing or preventing the reperfusion-induced endothelial injury and vascular leakage. Previous reports have also reported that AMPK plays a central role in different biological pathways, which makes this protein an attractive target for drug discovery against a variety of diseases like diabetes, obesity, atherosclerosis, and cancer (Zhang et al., 2009; Motoshima et al.,

2006). Based on the recent preliminary results in preclinical models, there must be a clear and focused effort to develop and identify potent and selective AMPK activators for the therapeutic use in humans afflicted with various types of pathological conditions.

## 6. References

Alexander JS, Hechtman HB, Shepro D (1988). Phalloidin enhances endothelial barrier function and reduces inflammatory permeability in vitro. Microvasc Res; 35: 308–315.

Beauloye C, Bertrand L, Horman S, Hue L (2011). AMPK activation, a preventive therapeutic target in the transition from cardiac injury to heart failure. Cardiovasc Res; 90: 224–233.

Beis I, Newsholme EA (1975). The contents of adenine nucleotides, phosphagens and some glycolytic intermediates in resting muscles from vertebrates and invertebrates. J Biochem; 152: 23–32.

Bhamra GS, Hausenloy DJ, Davidson SM, Carr RD, Paiva M, Wynne AM (2008). Metformin protects the ischemic heart by the Akt-mediated inhibition of mitochondrial permeability transition pore opening. Basic Res Cardiol; 103: 274–284.

Birukova AA, Smurova K, Birukov KG, Kaibuchi K, Garcia JG, Verin AD (2004). Role of Rho GTPases in thrombin-induced lung vascular endothelial cells barrier dysfunction. Microvasc Res; 67: 64–77.

Blume C, Benz PM, Walter U, Ha J, Kemp BE, Renne T (2007). AMP-activated protein kinase impairs endothelial actin cytoskeleton assembly by phosphorylating vasodilator-stimulated phosphoprotein. J Biol Chem; 282: 4601–4612.

Bogatcheva NV, Verin AD (2008). The role of cytoskeleton in the regulation of vascular endothelial barrier function. Microvasc Res; 76: 202–207.

Bonventre JV (1993). Mechanisms of ischemic acute renal failure. Kidney Int; 43: 1160-1178.

Calvert JW, Gundewar S, Jha S, Greer JJ, Bestermann WH, Tian R (2008). Acute metformin therapy confers cardioprotection against myocardial infarction via AMPK-eNOS-mediated signaling. Diabetes; 57: 696–705.

Carling D (2004). The AMP-activated protein kinase cascade – a unifying system for energy control. Trends Biochem Sci; 29: 18–24.

Celermajer DS, Sorensen KE, Gooch VM, Spiegelhalter DJ, Miller OI, Sullivan ID, Lloyd JK, Deanfield JE (1992). Non-invasive detection of endothelial dysfunction in children and adults at risk of atherosclerosis. Lancet; 340: 111–1115.

Corton JM, Gillespie JG, Hardie DG (1994). Role of the AMP activated protein kinase in the cellular stress response. Curr Biol; 4: 315–324.

Creighton J, Jian M, Sayner S, Alexeyev M, Insel PA (2011). Adenosine monophosphate-activated kinase {alpha} 1 promotes endothelial barrier repair. FASEB J; 25: 3356-3365.

Crute BE, Seefeld K, Gamble J, Kemp BE, Witters LA (1998). Functional domains of the a1 catalytic subunit of the AMP-activated protein kinase. J Biol Chem; 273: 35347–35354.

Daugherty RL, Gottardi CJ (2007). Phospho-regulation of ß-Catenin Adhesion and Signaling Functions. Physiology; 22: 303-309.

Davies JK, Wells DJ, Liu K, Whitrow HR, Daniel TD, Grignani R, Lygate CA, Schneider JE, Noel G, Watkins H, Carling D (2006). Characterization of the role of gamma2 R531G mutation in AMP-activated protein kinase in cardiac hypertrophy and Wolff-Parkinson-White syndrome. Am J Physiol Heart Circ Physiol; 290: H1942–H1951.

Dejana E, Orsenigo F, Lampugnani MG (2008). The role of adherens junctions and VE-cadherin in the control of vascular permeability. J Cell Sci; 121: 2115-2122.

Depre C, Wang L, Sui X, Qiu H, Hong C, Hedhli N, Ginion A, Shah A, Pelat M, Bertrand L, Wagner T, Gaussin V, Vatner SF (2006). H11 kinase prevents myocardial infarction by preemptive preconditioning of the heart. Circ Res; 98: 280–288.

Di Napoli P, Antonio Taccardi A, Grilli A, Spina R, Felaco M, Barsotti A, De Caterina R (2001). Simvastatin reduces reperfusion injury by modulating nitric oxide synthase expression: an ex vivo study in isolated working rat hearts. Cardiovasc Res; 51: 283–293.

Dixit M, Bess E, Fisslthaler B, Härtel FV, Noll T, Busse R, Fleming I (2008). Shear stress-induced activation of the AMP-activated protein kinase regulates FoxO1a and angiopoietin-2 in endothelial cells. Cardiovasc Res; 77: 160–168.

Dongaonkar RM, Stewart RH, Geissler HJ, Laine GA (2010). Myocardial microvascular permeability, interstitial oedema, and compromised cardiac function. Cardiovasc Res; 87:331-339.

Draijer R, Atsma DE, van der Laarse A, van Hinsbergh VW (1995). cGMP and nitric oxide modulate thrombin-induced endothelial permeability. Regulation via different pathways in human aortic and umbilical vein endothelial cells. Circ Res; 76: 199–208.

Dudek SM, Garcia JG (2001). Cytoskeletal regulation of pulmonary vascular permeability. J Appl Physiol; 91: 1487–1500.

Ermert L, Bruckner H, Walmrath D, Grimminger F, Aktories K, Suttorp N, Duncker HR, Seeger W (1995). Role of endothelial cytoskeleton in high-permeability edema due to botulinum C2 toxin in perfused rabbit lungs. Am J Physiol Lung Cell Mol Physiol; 268: L753–L761.

Ermert L, Duncker HR, Bruckner H, Grimminger F, Hansen T, Rossig R, Aktories K, Seeger W (1997). Ultrastructural changes of lung capillary endothelium in response to botulinum C2 toxin. J Appl Physiol; 82: 382–388.

Eto M, Ohmori T, Suzuki M, Furuya K, Morita F (1995). A novel protein phosphatase-1 inhibitory protein potentiated by protein kinase C. Isolation from porcine aorta media and characterization. J Biochem; 118: 1104–1107.

Fasano A, Fiorentini C, Donelli G, Uzzau S, Kaper JB, Margaretten K, Ding X, Guandalini S, Comstock L, Goldblum SE (1995). Zonula occludens toxin modulates tight junctions through protein kinase C-dependent actin reorganization, in vitro. J Clin Invest; 96: 710–720.

Feng J, Ito M, Ichikawa K, Isaka N, Nishikawa M, Hartshorne DJ (1999). Inhibitory phosphorylation site for Rho-associated kinase on smooth muscle myosin phosphatase. J Biol Chem; 274: 37385–37390.

Fernandez A, Brautigan DL, Mumby M, Lamb NJC (1990). Protein phosphatase Type-I, not Type-24 modulates acdn microfilament integrity and myosin light chain phosphorylation in living nonmuscle cells. J Cell Biol; 111: 103–112.

Fukata Y, Amano M, Kaibuchi K (2001). Rho-Rho-kinase pathway in smooth muscle contraction and cytoskeletal reorganization of non-muscle cells. Trends Pharmacol Sci; 22: 32–39.

Fürst R, Bubik MF, Bihari P, Mayer BA, Khandoga AG, Hoffmann F, Rehberg M, Krombach F, Zahler S, Vollmar AM (2008). Atrial natriuretic peptide protects against histamineinduced endothelial barrier dysfunction *in vivo*. Mol Pharmacol; 74: 1-8.

Garcia JG, Liu F, Verin AD, Birukova A, Dechert MA, Gerthoffer WT, Bamberg JR, English D (2001). Sphingosine 1-phosphate promotes endothelial cell barrier integrity by Edg-dependent cytoskeletal rearrangement. J Clin Invest; 108: 689–701.

Garcia-Dorado D, Piper HM (2006). Postconditioning: Reperfusion of reperfusion injury after hibernation. Cardiovasc Res; 69:1-3.

Garcia JG, Davis HW, Patterson CE (1995). Regulation of endothelial cell gap formation and barrier dysfunction: role of myosin light chain phosphorylation. J Cell Physiol; 163: 510–522.

Garcia JG, Lazar V, Gilbert-McClain LI, Gallagher PJ, Verin AD (1997). Myosin light chain kinase in endothelium: molecular cloning and regulation. Am J Respir Cell Mol Biol; 16: 489–494.

Gaskin F, Kamada K, Yusof M, Korthuis R (2007). 5'-AMP-activated protein kinase activation prevents postischemic leukocyte-endothelial cell adhesive interactions. Am J Physiol Heart Circ Physiol; 292: H326–H332.

Goirand F, Solar M, Athea Y, Viollet B, Mateo P, Fortin D, Leclerc J, Hoerter J, Ventura-Clapier R, Garnier A (2007). Activation of AMP kinase alpha1 subunit induces aortic vasorelaxation in mice. J Physiol; 581: 1163–1171.

Goeckeler ZM, Wysolmerski RB (1995). Myosin light chain kinase-regulated endothelial cell contraction: the relationship between isometric tension, actin polymerization, and myosin phosphorylation. J Cell Biol; 130:613-627.

Gundewar S, Calvert JW, Jha S, Toedt-Pingel I, Ji SY, Nunez D, Ramachandran A, Anaya-Cisneros M, Tian R, Lefer DJ (2009). Activation of AMP-Activated protein kinase by metformin improves left ventricular function and survival in heart failure. Circ Res; 104: 403–411.

Gündüz D, Kasseckert SA, Härtel FV, Aslam M, Abdallah Y, Schäfer M, Piper HM, Noll T, Schäfer C (2006). Accumulation of extracellular ATP protects against acute reperfusion injury in rat heart endothelial cells. Cardiovasc Res; 71: 764–773.

Hansen PR (1995). Myocardial reperfusion injury: experimental evidence and clinical relevance. Eur Heart J; 16: 734–740.

Hardie DG (2007). AMP-activated/SNF1 protein kinases: Conserved guardians of cellular energy. Nat Rev Mol Cell Biol; 8: 774–785.

Hardie DG (2004). The AMP-activated protein kinase pathway—new players upstream and downstream. J Cell Sci; 117: 5479–5487.

Hardie DG, Scott JW, Pan DA, Hudson ER (2003). Management of cellular energy by the AMP-activated protein kinase system. FEBS Lett; 546: 113–120.

Härtel FV, Rodewald CW, Aslam M, Gündüz D, Hafer L, Neumann J, Piper HM, Noll T (2007). Extracellular ATP induces assembly and activation of the myosin light chain phosphatase complex in endothelial cells. Cardiovasc Res; 74: 487–496.

Hartshorne DJ (1998). Myosin phosphatase: subunits and interactions. Acta Physiol Scand; 164: 483–493.

Hartshorne DJ, Ito M, Erdödi F (1998). Myosin light chain phosphatase: subunit composition, interactions and regulation. J Muscle Res Cell Motil; 19: 325–341.

Hawley SA, Davison M, Woods A, Davies SP, Beri RK, Carling D, Hardie DG (1996). Characterization of the AMP-activated protein kinase kinase from rat liver, and identification of threonine-172 as the major site at which it phosphorylates and activates AMP-activated protein kinase. J Biol Chem; 271: 27879-27887.

Hempel A, Noll T, Bach C, Piper HM, Willenbrock R, Hohnel K (1998). Atrial natriuretic peptide clearance receptor participates in modulating endothelial permeability. Am J Physiol; 275: H1818–H1825.

Hixenbaugh EA (1997). Stimulated neutrophils induce myosin light chain phosphorylation and isometric tension in endothelial cells. Am J Physiol; 273: H981–H988.

Hubbard MJ, Cohen P (1993). On target with a new mechanism for the regulation of protein phosphorylation. Trends Biochem Sci; 18: 172-177.

Hurley RL, Anderson KA, Franzone JM (2005). The $Ca^{2+}$/calmodulin-dependent protein kinase kinases are AMP-activated protein kinase kinases. J Biol Chem; 280: 29060–29066.

Ido Y, Carling D, Ruderman N (2002). Hyperglycemia-induced apoptosis in human umbilical vein endothelial cells: inhibition by the AMP-activated protein kinase activation. Diabetes; 51: 159–167.

Inauen W, Payne DK, Kvietys PR, Granger DN (1990). Hypoxia/reoxygenation increases the permeability of endothelial cell monolayers: role of oxygen radicals. Free Radic Biol Med; 9: 219–223.

Ito M, Nakano T, Erdodi F, Hartshorne DJ (2004). Myosin phosphatase: structure, regulation and function. Mol Cell Biochem; 259: 197–209.

Jaffe EA, Nachman RL, Becker CG, Minnick RC (1973). Culture of human endothelial cells derived from umbilical veins. J Clin Invest; 52: 2745–2756.

Johnson D, Cohen P, Chen MX, Chen YH, Cohen PT (1997). Identification of the regions on the M110 subunit of protein phosphatase 1M that interact with the M21 subunit and with myosin. Eur J Biochem; 244: 931–939.

Johnson LN, Noble MEM, Owen DJ (1996). Active and inactive protein kinases: structural basis for regulation. Cell; 85: 149–158.

Kahles H, Mezger VA, Hellige G, Spieckermann PG, Bretschneider HJ (1982). The influence of myocardial edema formation on the energy consumption of the heart during aerobiosis and hypoxia. Basic Res Cardiol; 77: 158–169.

Kamisoyama H, Araki Y, Ikebe M (1994). Mutagenesis of thre phosphorylation site (serine 19) of smooth muscle myosin regulatory light chain and its effects on the properties of myosin. Biochem; 33: 840–847.

Kasseckert SA, Schäfer C, Kluger A, Gligorievski D, Tillmann J, Schlüter KD, Noll T, Sauer H, Piper HM, Abdallah Y (2009). Stimulation of cGMP signaling protects coronary endothelium against reperfusion-induced intercellular gap formation. Cardiovasc Res; 83: 381–387.

Katakam PV, Ujhelyi MR, Hoenig M, Miller AW (2000). Metformin improves vascular function in insulin-resistant rats. Hypertension; 35: 108–112.

Khaidakov M, Szwedo J, Mitra S, Ayyadevara S, Dobretsov M, Lu J, Mehta JL (2010). Anti-angiogenic and anti-mitotic effects of aspirin in hypoxia-reoxygenation modulation of LOX-1-NADPH oxidase axis as potential mechanism. J Cardiovasc Pharmacol; 56: 635-641.

Kim SM, Edward JM, Wright MT, Li J, Qi D, Atsina K, Zaha V, Sakamoto K, Young HL (2011). A small molecule AMPK activator protects the heart against ischemia–reperfusion injury. J Mol Cell Cardiol; 51: 24–32.

Khimenko PL, Moore TM, Wilson PS, Taylor AE (1996). Role of calmodulin and myosin light-chain kinase in lung ischemia-reperfusion injury. Am J Physiol Lung Cell Mol Physiol; 271: L121–L125.

Kimura K, Ito M, Amano M, Chihara K, Fukata Y, Nakafuku M, Yamamori B, Feng J, Nakano T, Okawa, K, Iwamatsu A, Kaibuchi K (1996). Regulation of myosin phosphatase by Rho and Rho-associated kinase (Rho-kinase). Science; 273: 245–248.

Kitazawa T, Takizawa N, Ikebe M, Eto M (1999). Reconstitution of protein kinase C–induced contractile $Ca^{2+}$ sensitization in triton X-100 demembranated rabbit arterial smooth muscle. J Physiol; 520: 139–152.

Kodiha M, Rassi JG, Brown CM, Stochaj U (2007). Localization of AMP kinase is regulated by stress, cell density, and signaling through the MEK-->ERK1/2 pathway. Am J Physiol Cell Physiol; 293: C1427–C1436.

Koh H, Chung J (2007). AMPK links energy status to cell structure and mitosis. Biochem Biophys Res Commun; 362: 789–792.

Kolodney MS, Wysolmerski RB (1992). Isometric contraction by fibroblasts and endothelial cells in tissue culture: a quantitative study. J Cell Biol; 117: 73–82.

Komarova YA, Mehta D, Malik AB (2007). Dual regulation of endothelial junctional permeability. Sci STKE; Issue 412: re8.

Kudo N, Barr AJ, Barr RL, Desai S, Lopaschuk GD (1995). High rates of fatty acid oxidation during reperfusion of ischemic hearts are associated with a decrease in malonyl-CoA levels due to an increase in 5'-AMP-activated protein kinase inhibition of acetyl-CoA carboxylase. J Biol Chem; 270: 17513–17520.

Lage R, Dieguez C, Vidal-Puig A, Lopez M (2008). AMPK: a metabolic gauge regulating whole-body energy homeostasis. Trends Mol Med; 14: 539–549.

Lampugnani MG, Dejana E (1997). Interendothelial junctions: structure, signaling and functional roles. Curr Opin Cell Biol; 9: 674–82.

Lee JH, Koh H, Kim M, Kim Y, Lee SY, Lee S, Shong J, Kim J, Chung J, Karess RE (2007). Energy-dependent regulation of cell structure by AMP-activated protein kinase. Nature; 447: 1017–1021.

Lee JS, Yoon KC, Na RK, Lee WK, Suh SK, Kim YS, Chang SY, Shin TS, Bang KB (2009). The preconditioning with AICAR protects against subsequent renal ischemia reperfusion injury. Korean J Nephrol; 28: 96–102.

Liao Y, Takashima S, Maeda N, Ouchi N, Komamura K, Shimomura I, Hori M, Matsuzawa Y, Funahashi T, Kitakaze M (2005). Exacerbation of heart failure in adiponectin-deficient mice due to impaired regulation of AMPK and glucose metabolism. Cardiovasc Res; 67: 705–713.

Li JM, Shah AM (2004). Endothelial cell superoxide generation: regulation and relevance for cardiovascular pathophysiology. Am J Physiol Regul Integr Comp Physiol; 287: R1014–1030.

Li NX, Song J, Zhang L, LeMaire AS, Hou XP, Zhang C, Coselli SJ, Chen L, Wang LX, Zhang Y, Shen HYP (2009). Activation of the AMPK-FOXO3 pathway reduces fatty acid-induced increase in intracellular reactive oxygen species by upregulating thioredoxin. Diabetes; 10: 2246–2257.

Lum H, Barr DA, Shaffer JR, Gordon RJ, Ezrin AM, Malik AB (1992). Reoxygenation of endothelial cells increases permeability by oxidant-dependent mechanisms. Circ Res; 70: 991–998.

Lum H, Malik AB (1994). Regulation of vascular endothelial barrier function. Am J Physiol; 267: L223–L241.

Lum H, Malik AB (1996). Mechanisms of increased endothelial Permeability. Can J Physiol Phannacol; 74: 787–800.

Lampugnani MG, Corada M, Caveda L, Breviario F, Ayalon O, Geiger B, Dejana E. (1995). The molecular organization of endothelial cell to cell junctions: differential association of plakoglobin, beta-catenin, and alpha-catenin with vascular endothelial cadherin (VE-cadherin). J Cell Biol;129: 203-217.

Lynch MJ, Grum CM, Gallagher KP, Boiling SF, Deeb GM, Morganroth ML. (1988). Xanthine oxidase inhibition attenuates ischemic-reperfusion lung injury. J Surg Res; 44: 538–544.

MacDonald JA, Eto M, Borman MA, Brautigan DL, Haystead TA (2001). Dual Ser and Thr phosphorylation of CPI-17, an inhibitor of myosin phosphatase, by MYPT-associated kinase. FEBS Lett; 493: 91–94.

Marsin AS, Bertrand L, Rider MH, Deprez J, Beauloye C, Vincent MF, van den Berghe G, Carling D, Hue L (2000). Phosphorylation and activation of heart PFK-2 by AMPK has a role in the stimulation of glycolysis during ischaemia. Curr Biol; 10: 1247–1255.

McDonald DM, Thurston G, Baluk P (1999). Endothelial gaps as sites for plasma leakage in inflammation. Microcirculation; 6: 7–22.

Mehta D, Malik AB (2006). Signaling mechanisms regulating endothelial permeability. Physiol Rev; 86: 279–367.

Merrill GF, Kurth EJ, Hardie DG & Winder WW (1997). AICA riboside increases AMP-activated protein kinase, fatty acid oxidation, and glucose uptake in rat muscle. Am J Physiol Endocrinol Metab; 273: E1107–E1112.

Michel CC, Curry FE (1999). Microvascular permeability. Physiol Rev; 79: 703-761.

Miller EJ, Li J, Leng L, McDonald C, Atsumi T, Bucala R, Young LH (2008). Macrophage migration inhibitory factor stimulates AMP-activated protein kinase in the ischaemic heart. Nature; 451: 578–582.

Mirouse V, Swick LL, Kazgan N, St Johnston D, Brenman JE (2007). LKB1 and AMPK maintain epithelial cell polarity under energetic stress. J Cell Biol; 177: 387–392.

Momcilovic M, Hong SP, Carlson M (2006). Mammalian TAK1 activates Snf1 protein kinase in yeast and phosphorylates AMPK *in vitro*. J Biol Chem; 281: 25336-25343.

Morrow VA, Foufelle F, Connell JM, Petrie JR, Gould GW, Salt IP (2003). Direct activation of AMP-activated protein kinase stimulates nitric-oxide synthesis in human aortic endothelial cells. J Biol Chem; 278: 31629–31639.

Motoshima H, Goldstein BJ, Igata M & Araki E (2006). AMPK and cell proliferation – AMPK as a therapeutic target for atherosclerosis and cancer. J Physiol; 574: *63*–71.

Moy AB, Shasby SS, Scott BD, Shasby DM (1993). The effect of histamine and cyclic adenosine monophosphate on myosin light chain phosphorylation in human umbilical vein endothelial cells. J Clin Invest; 92: 1198–1206.

Musi N, Fujii N, Hirshman MF, Ekberg I, Froberg S, Ljungqvist O, Thorell A, Goodyear LJ (2001). AMP-activated protein kinase is activated in muscle of subjects with type 2 diabetes during exercise. Diabetes; 50: 921–927.

Nakamura K, Koga Y, Sakai H, Homma K, Ikebe M (2007). cGMP-dependent relaxation of smooth muscle is coupled with the change in the phosphorylation of myosin phosphatase. Circ Res; 101: 712–722.

Navarro P, Caveda L, Breviario F, Mândoteanu I, Lampugnani MG, Dejana E (1996). Catenin dependent and independent functions of VE-cadherin. J Biol Chem; 270: 30965–30972.

Noll T, Muhs A, Besselmann M, Watanabe H, Piper HM. (1995) Initiation of hyperpermeability in energy-depleted coronary endothelial monolayers. Am J Physiol; 268: H1462-H1470

Noll T, Wozniak G, McCarson K, Haji MA, Metzner HJ, Inserte J, Kummer W, Hehrlein FW, Piper HM (1999). Effect of factor XIII on endothelial barrier function. J Exp Med; 189: 1373–1382.

Paiva M, Riksen NP, Davidson SM, Hausenloy DJ, Monteiro P, Gonçalves L, Providência L, Rongen GA, Smits P, Mocanu MM, Yellon DM (2009). Metformin *prevents myocardial reperfusion injury by activating the adenosine receptor.* J Cardiovasc Pharmacol; 53: 373–378.

Paiva MA, Gonçalves LM, Providência LA, Davidson SM, Yellon DM, Mocanu MM (2010). Transitory activation of AMPK at reperfusion protects the ischaemic-reperfused rat myocardium against infarction. Cardiovasc Drugs Ther; 24: 25–32.

Parker JC (2000). Inhibitors of myosin light chain kinase and phosphodiesterase reduce ventilator-induced lung injury. J Appl Physiol; 89: 2241–2248.

Patt A, Harken AH, Burton LK, Rodell TC, Piermattei D, Schorr WJ, Parker NB, Berger EM, Horesh IR, Terada LS, Linas SL, Cheronis JC, Repine JE (1988). Xanthine oxidase-derived hydrogen peroxide contributes to ischemia reperfusion-induced edema in gerbil brains. J Clin Invest; 81: 1556–1562.

Pearlstein DP, Ali MH, Mungai PT, Hynes KL, Gewertz BL, Schumacker PT. (2002). Role of mitochondrial oxidant generation in endothelial cell responses to hypoxia. Arterioscler Thromb Vasc Biol; 22: 566-576.

Phillips PG, Lum H, Malik AB, Tsan M (1989). Phallacidin prevents thrombin-induced increases in endothelial permeability to albumin. Am J Physiol Cell Physiol; 257: C562–C567.

Piper HM, Abdullah Z, Schäfer AC (2004). The first minutes of reperfusion: a window of opportunity for cardioprotection. Cardiovasc Res; 61: 365–371.

Plant S, Shand B, Elder P, Scott R (2008). Adiponectin attenuates endothelial dysfunction induced by oxidised low-density lipoproteins. Diab Vasc Dis Res; 5: 102–108.

Reffelmann T, Hale SL, Dow JS, Kloner RA (2003). No-reflow phenomenon persists long-term after ischemia/reperfusion in the rat and predicts infarct expansion. Circulation; 108: 2911-2917.

Rodrigues SF, Granger DN (2010). Role of blood cells in ischaemia-reperfusion induced endothelial barrier failure. Cardiovasc Res; 87:291-299.

Rubin LJ, Magliola L, Feng X, Jones AW, Hale CC (2005). Metabolic activation of AMP kinase in vascular smooth muscle. J Appl Physiol; 98: 296–306.

Rubboli A, Sobotka PA, Euler DE (1994). Effect of acute edema on left ventricular function and coronary vascular resistance in the isolated rat heart. Am J Physiol Heart Circ Physiol; 267: H1054–H1061.

Russell RR, Li J, Coven DL, Pypaert M, Zechner C, Palmeri M, Giordano FJ, Mu J, Birnbaum MJ, Young LH (2004). AMP-activated protein kinase mediates ischemic glucose uptake and prevents postischemic cardiac dysfunction, apoptosis, and injury. J Clin Invest; 114: 495–503.

Sanders MJ, Grondin PO, Hegarty BD, Snowden MA, Carling D (2007). Investigating the mechanism for AMP activation of the AMP-activated protein kinase cascade. Biochem J; 403: 139–148.

Sartoretto JL, Melo GAN, Carvalho MHC, Nigro D, Passaglia RT, Scavone Cf, Cuman RKN, Fortes ZB (2005). Metformin treatment restores the altered microvascular reactivity in neonatal streptozotocin-induced diabetic rats increasing NOS activity, but not NOS expression. Life Sci; 77: 2676–2689.

Sasaki H, Asanuma H, Fujita M, Takahama H, Wakeno M, Ito S, Ogai A, Asakura M, Kim J, Minamino T, Takashima S, Sanada S, Sugimachi M, Komamura K, Mochizuki N, Kitakaze M (2009). Metformin prevents progression of heart failure in dogs: role of AMP-activated protein kinase. Circulation; 119: 2568–2577.

Scarabelli T, Stephanou A, Rayment N, Pasini E, Comini L, Curello S, Ferrari R, Knight R, Latchman D (2001). Apoptosis of endothelial cells precedes myocyte cell apoptosis in ischemia/reperfusion injury. Circulation; 104: 253-256.

Schäfer C, Walther S, Schafer M, Dieterich L, Kasseckert S, Abdallah Y, Piper HM (2003). Inhibition of contractile activation reduces reoxygenation-induced endothelial gap formation. Cardiovasc Res; 58: 149–155.

Schaphorst KL, Pavalko FM, Patterson CE, Garcia JG (1997). Thrombin-mediated focal adhesion plaque reorganization in endothelium: role of protein phosphorylation. Am J Respir Cell Mol Biol; 17: 443–455.

Schnittler HJ, Wilke A, Gress T, Suttorp N, Drenckhahn D (1990). Role of actin and myosin in the control of paracellular permeability in pig, rat and human vascular endothelium. J Physiol; 431: 379–401.

Scott JW, Hawley SA, Green KA, Anis M, Stewart G, Scullion GA, Norman DG, Hardie DG (2004). CBS domains form energy-sensing modules whose binding of adenosine ligands is disrupted by disease mutations. J Clin Invest; 113: 274-284.

Shasby DM, Shasby SS, Sullivan JM, Peach MJ (1982). Role of endothelial cell cytoskeleton in control of endothelial permeability. Circ Res; 51: 657–661.

Sheldon R, Moy A, Lindsley K, Shasby S, Shasby DM (1993). Role of myosin light-chain phosphorylation in endothelial cell retraction. Am J Physiol Lung Cell Mol Physiol; 265: L606–L612.

Shen Q, Wu MH, Yuan SY (2009). Endothelial contractile cytoskeleton and microvascular permeability. Cell Health Cytoskelet; 1: 43–50.

Shibata R, Sato K, Pimentel DR, Takemura Y, Kihara S, Ohashi K (2005). Adiponectin protects against myocardial ischemia reperfusion injury through AMPK-and COX-2-dependent mechanisms. Nat Med; 11: 1096–1103.

Shin EJ, Schram K, Zheng XL, Sweeney G (2009). Leptin attenuates hypoxia/reoxygenation-induced activation of the intrinsic pathway of apoptosis in rat H9c2 cells. J Cell Physiol; 221: 490–497.

Shinmura K, Tamaki K, Bolli R (2005). Short-term caloric restriction improves ischemic tolerance independent of opening of ATP-sensitive K+ channels in both young and aged hearts. J Mol Cell Cardiol; 39: 285–296.

Sidhu JS, Rajawat YS, Rami TG, Gollob MH, Wang Z, Yuan R, Marian AJ, DeMayo FJ, Weilbacher D, Taffet GE, Davies JK, Carling D, Khoury DS, Roberts R (2005). Transgenic mouse model of ventricular preexcitation and atrioventricular reentrant tachycardia induced by an AMP activated protein kinase loss-of-function mutation responsible for Wolff-Parkinson-White syndrome. Circulation; 111: 21–29.

Singleton PA, Dudek SM, Ma SF, Garcia JG (2006). Transactivation of sphingosine 1-phosphate receptors is essential for vascular barrier regulation. Novel role for hyaluronan and CD44 receptor family. J Biol Chem; 281: 34381–34393.

Singleton PA, Mirzapoiazova T, Guo Y, Sammani S, Mambetsariev N, Lennon FE, Moreno-Vinasco L, Garcia JG (2010). High-molecular-weight hyaluronan is a novel

inhibitor of pulmonary vascular leakiness. Am J Physiol Lung Cell Mol Physiol; 299: L639-L651.

Stein SC, Woods A, Jones NA, Davison MD, Carling D (2000). The regulation of AMP-activated protein kinase by phosphorylation. Biochem J; 345: 437–443.

Sukhodub A, Jovanović S, Du Q, Budas G, Clelland AK, Shen M, Sakamoto K, Tian R, Jovanovic A (2007). AMP-activated protein kinase mediates preconditioning in cardiomyocytes by regulating activity and trafficking of sarcolemmal ATP-sensitive K (+) channels. J Cell Physiol; 210: 224–236.

Torii H, Kubota H, Ishihara H, Suzuki M (2007). Cilostazol inhibits the redistribution of the actin cytoskeleton and junctional proteins on the blood-brain barrier under hypoxia/reoxygenation. Pharmacol Res; 55: 104–110.

Thorne GD, Ishida Y, Paul RJ (2004). Hypoxic vasorelaxation: $Ca^{2+}$-dependent and $Ca^{2+}$-independent mechanisms. Cell Calcium; 36: 201–208.

Tobacman LS, Korn ED (1983). The kinetics of actin nucleation and polymerization. J Biol Chem; 258: 3207–3214.

Towler MC, Hardie DG (2007). AMP-activated protein kinase in metabolic control and insulin signaling. Circ Res; 100: 328–341.

Velasco G, Armstrong C, Morrice N, Frame S, Cohen P (2002). Phosphorylation of the regulatory subunit of smooth muscle protein phosphatase 1M at Thr 850 induces its dissociation from myosin. FEBS Lett; 527: 101–104.

Verin AD, Gilbert-McClain LI, Patterson CE, Garcia JG (1998). Biochemical regulation of the nonmuscle myosin light chain kinase isoform in bovine endothelium. Am J Respir Cell Mol Biol; 19: 767–776.

Verin AD, Patterson CE, Day MA, Garcia JG (1995). Regulation of endothelial cell gap formation and barrier function by myosin-associated phosphatase activities. Am J Physiol; 269: L99–L108.

Verin AD, Wang P, Garcia JG (2000). Immunochemical characterization of myosin-specific phosphatase 1 regulatory subunits in bovine endothelium. J Cell Biochem; 76: 489–498.

Vouret-Craviari V, Boquet P, Pouyssegur J, Van Obberghen-Schilling E (1998). Regulation of the actin cytoskeleton by thrombin in human endothelial cells: role of Rho proteins in endothelial barrier function. Mol Biol Cell; 9: 2639–2653.

Vouret-Craviari V, Bourcier C, Boulter E, Van Obberghen-Schilling E (2002). Distinct signals via Rho GTPases and Src drive shape changes by thrombin and sphingosine-1-phosphate in endothelial cells. J Cell Sci; 115: 2475–2484.

Wang Y, Gao E, Tao L, Lau WB, Yuan Y, Goldstein BJ, Lopez BL, Christopher TA, Tian R, Koch W, Ma XL (2009). AMP-activated protein kinase deficiency enhances myocardial ischemia/reperfusion injury but has minimal effect on the antioxidant/antinitrative protection of adiponectin. Circulation; 119: 835–844.

Wang S, Liang B, Viollet B, Zou HM (2011). Inhibition of the AMP-activated protein kinase-α2 accentuates agonist-induced vascular smooth muscle contraction and high blood pressure in mice. Hypertension; 57: 1010–1017.

Wainwright MS, Rossi J, Schavocky J, Crawford S, Steinhorn D, Velentza AV, Zasadzki M (2003). Protein kinase involved in lung injury susceptibility: evidence from enzyme isoform genetic knockout and in vivo inhibitor treatment. Proc Natl Acad Sci USA; 100: 6233–6238.

Warden S, Richardson C, O'Donnell J, Stapleton D, Kemp B, Witters L (2001). Post-translational modifications to the beta-1 subunit of the AMP-activated protein kinase affect enzyme activity and cellular localization. Biochemistry; 354: 275–283.

Wardle RL, Gu M, Ishida Y, Paul RJ (2006). $Ca^{2+}$-desensitizing hypoxic vasorelaxation: pivotal role for the myosin binding subunit of myosin phosphatase (MYPT1) in porcine coronary artery. J Physiol; 572: 259–267.

Willert K, Nusse R (1998). β-Catenin: a key mediator of Wnt signaling. Curr Opin Genet Dev; 8: 95–102.

Winder WW, Hardie DG (1996). Inactivation of acetyl-CoA carboxylase and activation of AMP-activated protein kinase in muscle during exercise. Am J Physiol; 270: E299–E304.

Winder WW, Hardie DG (1999). AMP-activated protein kinase, a metabolic master switch: possible roles in type 2 diabetes. Am J Physiol; 277: 1–10.

Witt KA, Mark KS, Hom S, Davis TP (2003). Effects of hypoxia-reoxygenation on rat blood-brain barrier permeability and tight junctional protein expression. Am J Physiol Heart Circ Physiol; 285: H2820–H2831.

Woods A, Dickerson K, Heath R, Hong SP, Momcilovic M, Johnstone SR, Carlson M, Carling D (2005). $Ca^{2+}$/calmodulin-dependent protein kinase kinase-beta acts upstream of AMP-activated protein kinase in mammalian cells. Cell Metab; 2: 21–33.

Wysolmerski RB, Lagunoff D (1990). Involvement of myosin light chain kinase in endothelial cells retraction. Proc Nat Acad Sci USA; 87: Regulation of permeabilized endothelial cell retraction by myosin phosphorylation. Am J Physiol Cell Physiol; 261: C32–C40.

Yang W, Hong YH, Shen X, Frankowski C, Camp HS, Leff T (2001). Regulation of transcription by AMP-activated protein kinase. J Biol Chem; 276: 38341–3834.

Yuan SY, Huang Q, Wu HM (1997). Myosin light chain phosphorylation: modulation of basal and agonist-stimulated venular permeability. Am J Physiol; 272: H1437–H1443.

Zhang BB, Zhou G, Li C (2009). AMPK: an emerging drug target for diabetes and the metabolic syndrome. Cell Metab; 9: 407–416.

Zhang J, Bian HJ, Li XX, Liu XB, Sun JP, Li N, Zhang Y, Ji XP (2010). ERK-MAPK signaling opposes rho-kinase to reduce cardiomyocyte apoptosis in heart ischemic preconditioning. Mol Med; 16: 307–315.

Zhang L, Li J, Young LH, Caplan MJ (2006). AMP-activated protein kinase regulates the assembly of epithelial tight junctions. Proc Natl Acad Sci USA; 103: 17272–17277.

Zhang M, Dong Y, Xu J, Xie Z, Wu Y, Song P, Guzman M, Wu J, Zou MH (2008). Thromboxane receptor activates the AMP-activated protein kinase in vascular smooth muscle cells via hydrogen peroxide. Circ Res; 102: 328–337.

Zhang Y, Lee TS, Kolb EM, Sun K, Lu X, Sladek FM, Kassab GS, Garland T Jr, Shyy JY (2006). AMP-activated protein kinase is involved in endothelial NO synthase activation in response to shear stress. Arterioscler Thromb Vasc Biol; 26: 1281–1287.

Zhao J, Yue W, Zhu MJ, Sreejayan N, Du M (2010). AMP-activated protein kinase (AMPK) cross-talk with canonical Wnt signaling via phosphorylation of b-catenin at Ser 552. Biochem Biophys Res Commun; 395: 146–151.

Zheng B, Cantley LC (2007). Regulation of epithelial tight junction assembly and disassembly by AMP-activated protein kinase. Proc Natl Acad Sci USA; 104: 819–822.

## 7. Summary

Capillary leakage and edema formation is a complication of hypoxia and/or ischemia, which can compromise the outcome of reperfusion and the recovery of organs. AMP-activated protein kinase (AMPK) is an intracellular energy sensor, which regulates cellular metabolism to maintain the energy homeostasis. Recent studies, however, show that AMPK plays an important role in other physiological functions. Here the hypothesis was addressed whether AMPK is involved in the regulation of endothelial barrier function and a targeted activation of AMPK at the onset of reperfusion can protect against reperfusion-induced endothelial barrier failure. Therefore, the role of AMPK in endothelial barrier function was analyzed in human umbilical vein endothelial cells under physiological and pathophysiological (hypoxia-reperfusion) conditions. It was found that the downregulation of AMPKα protein or its isoforms (α1 and α2) with siRNA resulted in a significant increase in basal permeability, disintegration of adherens junctions, and enhanced actin stress fiber formation in cultured endothelial monolayers. Exposure of endothelial cells to hypoxia (60 min, $Po_2$<5 mmHg) led to an increase in interendothelial gap formation, activation of the contractile machinery (MLC and MYPT1 phosphorylation), F-actin stress fiber formation, and loss of VE-cadherin and β-catenin from cell-cell junctions. These parameters were further aggravated during reperfusion. Moreover, reperfusion also elicited translocation of both AMPKα isoforms from cytoplasm to the nucleus. Hypoxia caused a marked increase in AMPK phosphorylation which is associated with activation of the enzyme, however during reperfusion AMPK phosphorylation declined rapidly. Targeted activation of AMPK by the adenosine analog AICAR at the onset of reperfusion reduced interendothelial gap formation. Simultaneously MLC and MYPT1 phosphorylation was abolished, cortical actin rearranged at cell borders, VE-cadherin/β-

catenin re-established at cell junctions, and cytonuclear translocation of AMPKα isoforms was prevented. This protective effect of AICAR on all parameters was abolished by the AMPK inhibitor Ara-A or by AMPKα1/2 siRNA transfection. In isolated reperfused mouse hearts, pharmacological activation of AMPK led to a significant reduction in ischemia-reperfusion induced increase in water content denoting reduction of edema formation. The data of this study show that AMPK is involved in the regulation of endothelial barrier function. Targeted activation at the onset of reperfusion can protect against ischemia/hypoxia-reperfusion induced endothelial barrier failure. Therefore, activation of AMPK may be a promising new therapeutic option to prevent reperfusion-induced endothelial barrier dysfunction.

## 8. Zusammenfassung

Kapilläre Leckage und Ödembildung sind Komplikationen die bei Hypoxie und/oder Ischämie auftreten und den Ausgang der Reperfusion und die Erholung von Organen kompromittieren können. Die AMP-aktivierte Kinase (AMPK) ist ein intrazellulärer Sensor der den zellulären Metabolismus reguliert um die energetische Homöostase zu gewährleisten. Neuere Studien zeigen jedoch, dass die AMPK eine wichtige Rolle in Bezug auf andere physiologische Funktionen erfüllt. Hier wurde die Hypothese geprüft, ob die AMPK an der Regulation der endothelialen Schrankenfunktion beteiligt ist und ob eine AMPK gezielte Aktivierung zu Beginn der Reperfusion kann gegen Reperfusion-induziertes Schrankenversagen schützen. Zu diesem Zweck wurde die Rolle der AMPK in Bezug auf die endotheliale Schrankenfunktion in humanen Endothelzellen aus Nabelschnurvenen unter physiologischen und pathophysiologischen (Hypoxie-Reperfusion) Aspekten untersucht. Es fand sich, dass die Verminderung der AMPKα bzw. ihrer Isofomen (α1 und α2) mittels siRNA in einem signifikanten Anstieg der basalen Permeabilität, einer Disintegration von Adherens Junctions und einem Anstieg von Stressfaserbildung einherging. Aussetzen von Endothelzellen einer Hypoxie (60 min, $Po_2$ < 5 mmHg) führte zu einem Anstieg interendothelialer Lückenbildung, Aktivierung des kontraktilen Apparates (MLC und MYPT1 Phosphorylierung), F-Aktin Stressfaser-Bildung und Verlußt von VE-Cadherin und β-Catenin an Zellverbindungen. Diese Parameter verschlechterten sich im Verlaufe der Reperfusion. Darüberhinaus konnte eine Translokation beider AMPKα-Isoformen vom Zytoplasma in die Zellkerne beobachtet werden. Hypoxie induzierte einen Anstieg der AMPK Phosphorylierung, welche mit einer Aktivierung des Enzyms einhergeht, allerdings verschwindet diese Phosphorylierung während der Reperfusion rasch. Die gezielte Aktivierung der AMPK durch

das Adenosinanalog AICAR zu Beginn der Reperfusion verminderte die interendotheliale Lückenbildung. Gleichzeitig wurde die Phosphorylierung von MLC und MYPT1 verhindert, kortikales Aktin ordnete sich ebenso wie VE-Cadherin/β-Catenin an Zellgrenzen erneut an und die Kerntranslokation der AMPKα-Isoformen wurde verhindert. Dieser protektive Effekt von AICAR auf alle gemessenen parameter wurde jedoch durch den AMPK-Inhibitor Ara-A bzw. AMPKα1/2 siRNA Transfektion verhindert. In isolierten reperfundierten Mausherzen führte die pharmakologische Aktivierung von AMPK zu einer signifikanten Verminderung der Ischämie-Reperfusion induzierten Wassereinlagerung in das Gewebe, was eine Verminderung der Ödembildung kennzeichnet. Die Daten dieser Studie zeigen, dass AMPK an der Regulation der endothelialen Schrankenfunktion beteiligt ist. Die gezielte Aktivierung zu Beginn der Reperfusion kann gegen Ischämie/Hypoxie-Reperfusion induziertes Schrankenversagen schützen. Aus diesem Grund stellt die Aktivierung der AMPK eine mögliche neue therapeutische Option gegen reperfusions-induziertes endotheliales Schrankenversagen dar.

## 9. Declaration

"I declare that I have completed this dissertation single-handedly without the unauthorized help of a second party and only with the assistance acknowledged therein. I have appropriately acknowledged and referenced all text passages that are derived literally from or are based on the content of published or unpublished work of others, and all information that relates to verbal communications. I have abided by the principles of good scientific conduct laid down in the charter of the Justus Liebig University of Giessen in carrying out the investigations described in the dissertation."

Muhammad Assad Riaz

## 10. Acknowledgements

I would first and foremost like to express my heartfelt gratitude to my project supervisor Prof. Dr. Thomas Noll who had confidence in me and allowed me to contribute to the laboratory. I am so grateful for his invaluable guidance, patience and perseverance, which made this degree challenging and very rewarding.

I feel very fortunate to have the close association of former director of the Institute of Physiology, Prof. Dr. Dr. H. M. Piper whose influencing personality provided an inspiration to me. I also extend my deepest thanks to the director of Institute of Physiology, Prof. Dr. Rainer Schulz, for providing me a place in the Institute to carry on my PhD project.

I would like to sincerely thank Dr. Frauke Härtel whose approachability and positive criticism in the project greatly speeded up the progress of my work.

I extend my gratitude to Prof. Dr. Andreas Deussen for kindly allowing me to practice *ex vivo* studies in his lab. Additionally, I am very thankful to all the members of his research group, especially Anett Jannasch for helping in the *ex vivo* study on Langendorff-perfused mouse hearts.

Special thanks go to Hermann Holzträger, Anna Reis and Annika Krautwurst for their technical assistance.

I would especially like to thank Dr. Shaaban S Mousa, for his encouragement, insightful advice, and constructive feedback during the entire period of research work. Dear Mr. and Mrs. Arshad thanks for your friendship, support and for all the fun stuff we have done together.

I am also thankful to all members of my lab, especially Aslam, Daniel, Tatyana, Krishna, Sabiha, Kiran, Imran, Anupam and Adrian for providing a nice atmosphere in the lab. I am also grateful to all the scientific, parascientific and administrative staff of the Institute of Physiology, Giessen who were directly or indirectly involved in my research work.

No words can express the love and support that my parents and my brothers, sisters, and great Anwaiz chachoo extended to me throughout my life and I love you all from bottom of my heart. Last, but certainly not least, my wife who holds a special place in my heart, has been with me throughout this entire journey and her love, quiet patience and strength have led me through these less tread roads.

**Der Lebenslauf wurde aus der elektronischen Version der Arbeit entfernt.**

**The curriculum vitae was removed from the electronic version of the paper.**

## 12. Publications

(1) Amer Riazuddin, Afshan Yasmeen, Wenliange Yao, Yuri V. Sergeen, Qingiong Zhang, Freeha Zulfiqar, **Assad Riaz**, Fieling Hejtmancik (2005). Mutation in BB3-crystallin associated with autosomal Recessive Cataract in two Pakistani families. Invest Ophthalmol Vis Sci; 46: 2100-2106.

**Chapter in book:**

Rashid Mehmood, Muhammad Ramzan, Akhtar Ali, **Assad Riaz**, Fareeha Zulfiqar, Sheikh Riazuddin "Identification of genes causing recessive Retinitis pigmentosa, in Gene Therapy: prospective technology assessment in its social context" (2006) (editors J.Niewohner & C.Tannert), Elsevier Press, Amsterdam, The Netherlands & Oxford, UK. Vol: Section I, Scientific Aspects, Chapter 1 pp: 03-12 (Book)

**Abstracts published**

(1) **Assad M**, Arshad M, Haertel FV, Aslam M, Fleming I, Piper H M, Noll T (2008). Role of AMP-activated Protein Kinase in Ischemia-Reperfusion-Induced Barrier Failure in Endothelial Monolayers. Circulation, 2008; 118: S-575 Abstract 5509 (American Heart Association Scientific sessions 2008, New Orleans, USA).

(2) **Assad M**, Arshad M, Hartel FV, Aslam M, Fleming I, Piper H M, Noll T (2009). Activation of AMP-activated protein kinase protects endothelial barrier against reperfusion-induced failure. J FASEB, 2009; 763.13 (Experimental Biology 2009, New Orleans, USA).

(3) **Assad M**, Arshad M, Haertel FV, Aslam M, Fleming I, Piper H M, Noll T (2009). Activation of AMP-activated Protein kinase protects endothelial barrier against reperfusion-induced failure.

Acta Physiologica, 2009; 195: S669 (88th Annual meeting of Deutsche Physiologische Gesellschaft 2009, Giessen, Germany).

(4) **Riaz M**, Arshad M, Haertel F, Aslam M, Fleming I, Piper HM, Noll T (2009). AMP-activated protein kinase protects endothelial barrier against reperfusion-induced failure (Annual meeting of European Society of Cardiology 2009, Barcelona Spain).

(5) Nazli S, Aslam M, Haertel F, **Riaz MA**, Noll T (2009). Activation of Endothelial Myosin Phosphatase via Inhibition of CPI-17 Ameliorates Reperfusion Induced Endothelial Barrier Failure. Circulation, 2009; 120: S-1162 (American Heart Association Scientific sessions 2009, Orlando, USA).

(6) **Assad M**, Härtel FV, Arshad M, Aslam M, Fleming I, Piper H M, Noll T (2009). Aktivierung der AMP-aktivierten proteinkinase schützt vor reperfusion-induziertem endothelialen Schrankenversagen. (75th Annual Meeting of German Cardiac society, April 2009, Mannheim, Germany).

(7) **Riaz MA**, Arshad M, Aslam M, Hartel F, Fisselthaler B, Fleming I, Piper HM, Noll T (2010). AMPK activation presents a novel therapeutic target against reperfusion-induced endothelial barrier failure. Acta Physiologica, 2010; 198: 677 (Joint Meeting of the Scandinavian and German Physiological Societies 2010, Copenhagen, Denmark).

(8) **Assad M**, Arshad M, Aslam M, Härtel FV, Fisselthaler B, Fleming I, Piper HM, Noll T (2010). AMPK activation presents a novel therapeutic target against reperfusion-induced endothelial barrier failure. (76th Annual Meeting of German Cardiac society, April 2010, Mannheim, Germany).

(9) Härtel FV, **Riaz MA**, Aslam M, Gündüz D, Noll T (2010). Activation of AMP-activated Protein Kinase Displays a Novel Strategy Against Reperfusion-Induced Barrier Failure in Endothelial

Cells. Circulation, 2010; 122: Abstract 19391 (American Heart Association Scientific sessions 2010, Chicago, USA).

**(10)** M Arshad, C Conzelmann, F Härtel, M Aslam, I Hussain, M Städtle, **MA Riaz,** DG Sedding, HM Piper, T Noll, D Gündüz (2011). Connexin 43 acts as a Counter Regulatory Molecule Of Caveolin- 1 In The Control Of Angiogenesis. (77th Annual Meeting of German Cardiac society, April 2011, Mannheim, Germany).

**(11)** M Arshad, M Städtle, M Aslam, I Hussain, **MA Riaz**, DG Sedding, Mehmet Bilgin, HM Piper, T Noll, D Gündüz (2011). Platelet Glycoprotein IIb/IIIa Receptor Controls the Pro-Angiogenic Effect of Platelet Releasate. Circulation 124: A 15903 (American Heart Association Scientific sessions 2011, Orlando FL, USA).